RC 22560 (W0209-058) September 13, 2002
Physics

IBM Research Report

"Dressed-Atom" Lasers in Space

P. P. Sorokin, J. H. Glownia
IBM Research Division
Thomas J. Watson Research Center
P.O. Box 218
Yorktown Heights, NY 10598

Research Division
Almaden - Austin - Beijing - Haifa - India - T. J. Watson - Tokyo - Zurich

Astronomy & Astrophysics manuscript no. lwi2cref August 1, 2002
(DOI: will be inserted by hand later)

"Dressed-atom" lasers in Space

P. P. Sorokin and J. H. Glownia

IBM Research Division, P. O. Box 218, Yorktown Heights, NY 10598, USA e-mail: sorokin@us.ibm.com, glownia@us.ibm.com

Received 22 July 2002; accepted

Abstract.

It is shown that a model recently proposed for two-level-atom lasers without inversion (LWI) in Space (Sorokin & Glownia 2002) gains significant credibility when the model is instead constructed on the basis of atoms simultaneously saturated on two atomic transitions sharing a common level. The principal advantage attained by considering the atoms in the model to have three active levels rather than two is that the efficiency of the pumping mechanism no longer rapidly decreases with increasing power of the coherently generated light beam(s). The powerful "dressed-atom" approach for analyzing the physics of atoms strongly driven by resonant light beams (Cohen-Tannoudji & Reynaud 1977) provides a direct and insightful way both to understand this effect and to deduce exactly which optical pumping mechanisms should be most effective in converting intense broadband continuum light into coherent radiation at the bare-atom resonance frequencies ω_o and ω_o' in three-level-atom gases situated near bright continuum-emitting sources.

For three-level dressed-atom lasers, linear optical pumping by the continuum light is shown to be generally ineffective, leaving two nonlinear processes, broadband stimulated Raman scattering (SRS) and stimulated hyper-Raman scattering (SHRS) to be considered as excitation mechanisms. However, only SHRS can account for the narrow-band emission intensity being significantly greater than the continuum background level. In space objects having very high electron densities, such as symbiotic stars, an additional nonlinear mechanism, stimulated hyper-Compton scattering (SHCS), is postulated to be operative. SHCS would enable efficient transfer of continuum photon energy to occur over very large spectral intervals. One can account for the very large peak-to-background intensity ratio observed for the O VI (1032 Å, 1038 Å) doublet emission in symbiotic stars only by postulating that both SHRS and SHCS occur in these systems.

On the basis of Doppler width considerations, it is further explained that a three-level atomic system has a very much greater chance of operating as a dressed-atom laser in Space if its bare-atom frequencies happen to lie very close together. This may help explain why the O VI doublet emission is so dominant in symbiotic stars.

Key words. atomic processes – radiation mechanisms: non-thermal – stars: individual: RR Tel

1. Introduction

In a recently published paper (Sorokin & Glownia 2002 - hereafter referred to as S&G I), a new idea was suggested to explain superintense narrow-band emission lines radiated by certain space objects. Specifically considered in S&G I were the powerful O VI (1032 Å, 1038 Å) doublet emission that dominates the far-UV (FUV) spectra of symbiotic stars such as RR Tel, and the sharp, anomalously strong, H(α) emission line that is occasionally seen in reddened, early-type stars. It was proposed that these emissions represent spherically expanding output beams of so-called “lasers without inversion (LWI)”- the latter being located near certain very bright stars and being pumped by the blackbody continuum light emitted by those stars. A reasonably complete discussion was presented in S&G I of the essential physics that underlies the operation of an LWI. In general, any viable LWI scheme must include a photonic process that produces complete transparency at the lasing frequency, a condition usually referred to as “electromagnetically induced transparency” or EIT. In addition, there must exist a credible pumping mechanism, as well as a well defined source of pumping energy.

In Sect. 4 of S&G I, a lengthy description was given of some of the techniques that have been developed for inducing EIT in three-level atomic systems. The relative energies and parity assignments of the atomic levels in a three-level-atom system determine whether it is to be classified as a “cascade”-type, “V”-type, or “Λ”-type system (Fig. 1). In each of these types, the parities of two of the levels are generally taken to be the same, with the third being opposite. (In the present paper this simple parity characterization of levels is assumed.) Two of the three transitions are thus dipole allowed; the third is dipole forbidden. In principle, it should be quite straightforward to establish a condition of EIT in a tenuous gas of three-level atoms in Space. As noted at the end of Sect. 4 in S&G I, “co-propagation of two resonantly-tuned, monochromatic laser beams through a tenuous gas of three-level atoms accomplishes one major step needed to realize an LWI in space - it removes in principle all attenuation (loss) for the two beams as they propagate away from stars that provide the pumping power required for amplification of the beams.” This induced transparency occurs less as a result of saturation (i.e. equalling of the populations in the upper and lower levels of an unperturbed atomic transition), and more through quantum interference. The two laser beams effectively drive all atoms of the gas into a stable “coherently phased population state”. In this state, the wavefunctions of all the atoms in the gas become linear combinations of the unperturbed (“bare-atom”) wavefunctions of the three levels. Atoms coherently phased by this method are also commonly referred to as “dressed atoms”, and sometimes also as “coherently trapped atoms”. (The latter term is especially appropriate for Λ-

Send offprint requests to: P. P. Sorokin

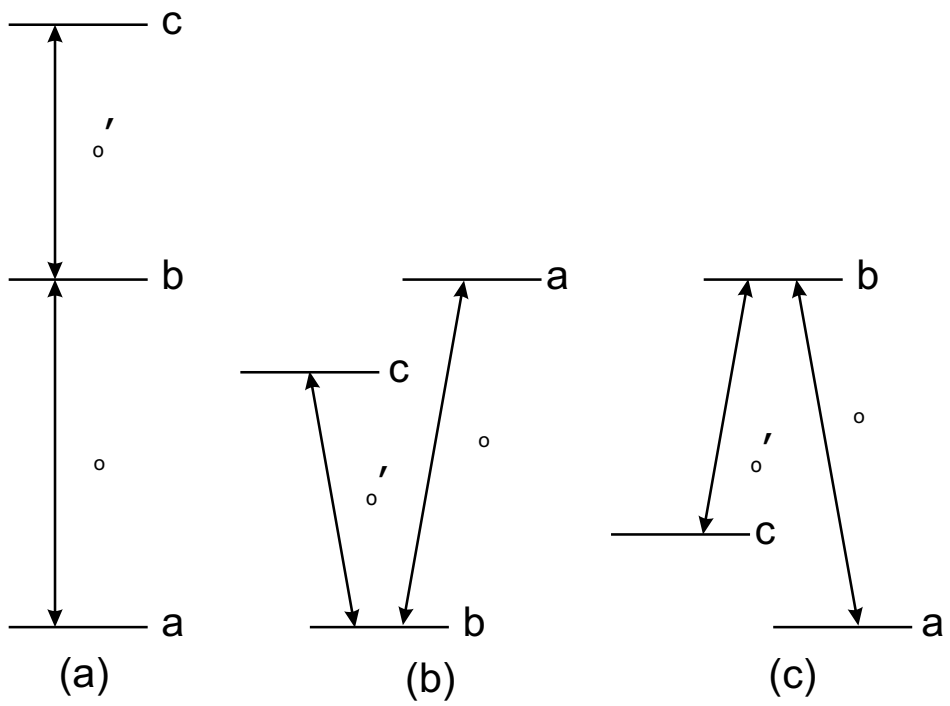

Fig. 1. Energy level structures for (a) cascade-, (b) V-, and (c) Λ-type three-level atoms.

type and V-type systems, as will be made clear below.) For reasons which will shortly be made apparent, the term “dressed atoms” is favored in the present paper.

Although the discussion in Sect. 4 of S&G I was entirely focussed on the establishment of EIT in three-level atomic systems, the need to find a credible pumping mechanism for an LWI in Space prompted the authors at that point to consider the possibility that an LWI might be realized with an even simpler system - a gas of two-level atoms. It was noted in S&G I that complete transparency in the vicinity of the resonance frequency ω_o of a two-level atom can be induced in a gas of such atoms simply by propagating through the gas a narrow-band laser beam tuned to ω_o. However, unlike what happens when EIT occurs in three-level atomic systems, EIT in two-level atomic systems is invariably accompanied by heavy saturation of the transition, which in turn leads to a rapid drop off in the efficiency of the stimulated hyper-Raman scattering (SHRS) process proposed as the LWI pumping mechanism in S&G I. This problem with the two-level-atom LWI scheme was fully recognized in S&G I, and it was proposed that, as the power in the beam at ω_o increases, a related resonant process, four-wave mixing (FWM), becomes the dominant nonlinear process that transfers power from the intense hot star continuum that irradiates the gas to the coherently generated beam at ω_o. However, the calculation given in Appendix A of S&G I showed that the FWM pumping process also strongly saturates, hinting that in future studies one might explore whether there exist modifications of the basic SHRS pumping scheme proposed in S&G I that can account for lasing in a space object that emits

narrow-band light at an intensity exceeding that of the surrounding continuum level by several orders of magnitude, e.g. as in each of the three symbiotic stars considered in S&G I.

The main goal of the present paper is to show that there indeed exists a simple modification of the basic SHRS pumping scenario proposed in S&G I that does allow continuum photons to be efficiently converted to narrow-band photons at very high power levels. Specifically, it will here be outlined that saturation of the output power of a space laser comprising a gas of *three-level* atoms can be completely avoided. The procedure here followed is to assume that, at a relatively small distance from the illuminating star, the two allowed atomic transitions are already being driven by intense monochromatic resonant laser light. It is next assumed that the same basic SHRS pumping mechanism discussed in S&G I here operates in the spectral vicinity of *each* transition, effectively converting continuum photons extracted from broad spectral ranges into narrow-band laser photons at both transition frequencies. It is shown that the structure of a three-level atom allows this “dual” SHRS pumping process to continue to operate with high efficiency, even at very high narrow-band laser light intensity levels. This implies that the monochromatic light assumed to be initially present at the two atomic frequencies becomes strongly amplified in propagating further and further from the illuminating star. While this line of reasoning displays to some extent a “chicken-before-the-egg” aspect, the strongly resonant nature and nonsaturability of the pumping transitions suggest that the narrow-band emissions are nonetheless able to evolve and grow in the presence of intense thermal continuum light.

Before seriously attempting to explain in detail the reasons why three-level atomic systems must be regarded as the most likely candidates for space lasers, we first review in Sect. 2 several spectral properties of the superintense O VI (1032 Å, 1038 Å) doublet emission lines that are seen in symbiotic stars. Such systems were one of two tentatively identified as possible LWIs in Space in S&G I. We have here chosen to focus entirely upon O VI-line-emitting symbiotic stars with our new space laser model, because their structures and astronomical environments appear to be better understood than those of other space objects emitting superintense emission lines. In the present paper we discuss archived spectral data obtained for these systems that could not easily be explained by the two-level-atom model employed in S&G I, and consequently were not discussed in that paper. This additional information includes spontaneous Raman scattering spectral data, a spectrum of the O VI doublet emission in RR Tel recorded at very high detector gain, and O VI doublet emission spectra in several symbiotic stars recorded with very high spectral resolution.

To a first approximation, one would expect an existing dressed-atom laser field in a symbiotic star system to originate near the part of the white dwarf surface that faces the red giant. This field should then propagate and become amplified in directions pointing radially away from the hot star surface and towards the cool giant. One would expect the field to have cylindrical symmetry about the line that joins the two stars, and to be largely confined within some angle θ about this line.

In analyzing Raman scattering in symbiotic stars, it simplifies matters to assume that the plane in which the stars orbit about one another is close to the plane of the sky, i.e. that the

symbiotic star system is viewed from Earth in quadrature. Since the intensely emitting D-type symbiotic star RR Tel is known to have such an orientation (Espey et al. 1995), an attempt is made in the present paper to show that, with a relatively simple model incorporating a dressed-atom laser, it is possible to account approximately for the observed FUV and Raman intensity spectra in this system, while maintaining consistency with consensus values of symbiotic star parameters that appear in Raman scattering models. For example, on the basis of the dressed-atom-laser model, it becomes necessary to explain how, when viewing RR Tel (or any symbiotic star, for that matter!) from Earth, it is possible to observe emission of intense light at 1032 Å and 1038 Å, since the dressed-atom laser field should be confined within some angle θ about the symbiotic star axis as it propagates from the hot star surface to the cool giant. On the basis of the explanation offered, it is shown how one can utilize O VI FUV doublet emission spectra of RR Tel recorded at very high gain to estimate the intensity of the generated laser light in this system, which should be hidden from our direct view for the reason just explained. The large intensity that is inferred provides a powerful constraint that leads to the conclusion made in Sect. 5 that the dominant pumping mechanism for O VI emission in symbiotic stars must necessarily involve SHRS occurring concomitantly with a second nonlinear process, stimulated hyper-Compton scattering (SHCS). SHCS serves to convert efficiently continuum photons with frequencies offset by thousands of wavenumbers from the bare-atom frequencies into photons with frequencies lying in the spectral vicinity of the latter. The photons produced via SHCS can then be converted by SHRS into narrow-band coherent light at the bare-atom frequencies. Since SHCS involves photon scattering by electrons, the transition probability is therefore proportional to the electron density n_e. In most current symbiotic star models, the value of n_e in the O VI region is assumed to be very high, on the order of 10^{10} cm^{-3}. Symbiotic stars are therefore space objects in which SHCS is *a priori* likely to occur.

To try to identify a mechanism which would allow a space laser beam to be amplified without saturation occuring, we have found it most helpful to use the powerful “dressed-atom” approach for analysis of resonantly driven three-level-atom systems, an approach that was proposed and explained in an illuminating paper published several years ago (Cohen-Tannoudji & Reynaud 1977 - hereafter referenced as C-T&R). This classical paper therefore forms the basis for Sect. 3 of the present paper. In that section, it is explained how one first constructs a foundation for the dressed-atom approach by considering an infinite lattice of “multiplicities” $\varepsilon_{n,n'}$ representing states of a system comprising an atom plus the two resonant laser fields with which it interacts. Each multiplicity consists of a threefold degenerate set of states. Each such state can be represented by a ket of the form $|\ l, n, n'\rangle$, corresponding to an atom in level l ($l = a, b, c$ - see Fig. 1) in the presence of n photons at ω_o and n' photons at ω'_o, with an unperturbed energy $E_l + n\omega_o + n'\omega'_o$ (taking $\hbar = 1$.). The threefold degenerate states comprising a given multiplic-

ity depend upon whether the three-level system being considered is of cascade-type, V-type, or Λ-type. For cascade-type systems (the only type explicitly considered in C-T&R), one has

$$\varepsilon_{n,n'} = \{|\, a, n+1, n'\rangle, |\, b, n, n'\rangle, |\, c, n, n'-1\rangle\}\,. \tag{1}$$

In the dressed-atom approach, one is really seeking to find the eigensolutions of the combined system of atom and monochromatic driving fields. The next step one takes is therefore to calculate how the multiplicities $\varepsilon_{n,n'}$ become perturbed by the presence of the two resonant laser beams at ω_o and ω_o'. A comparatively simple situation results when the so-called “secular approximation” is made, that is, when it is assumed that a quantity termed the “generalized Rabi frequency” Ω_1 is large compared to either of the radiative decay rates for the transitions *ab* and *bc*. (As already mentioned, it is here assumed that for all three types of atom structures the *ac* transition is radiatively forbidden.) In the presence of the resonant laser fields, each threefold degenerate multiplicity splits into three new states (the “dressed-atom” states) $|\, i, n, n'\rangle$ $(i = 1, 2, 3)$, with the separation in energy between adjacent states in a given multiplicity being $(1/2)\Omega_1$. From the expansions of the dressed-atom states as linear combinations of the bare-atom states, one can determine the rates of all possible spontaneous emission decays from the three perturbed states of $\varepsilon_{n,n'}$ to lower multiplicities, i.e. one can determine the fluorescence spectra $F_{ab}(\omega)$ and $F_{bc}(\omega)$ of the dressed-atom system. For cascade-type atoms, C-T&R show that each spectrum exhibits five equidistant Lorentzian components, with adjacent ones separated by $(1/2)\Omega_1$. C-T&R also show that (again, when the secular approximation holds) one can easily obtain expressions for the steady-state populations $\sigma_{ii}^{o}(n, n')$, which, to a very good approximation, can be factorized as:

$$\sigma_{ii}^{o}(n, n') = \{\pi_i\}\, p_o(n) p_o'(n') \tag{2}$$

where $p_o(n)$ and $p_o'(n')$ are the distributions of the photon numbers n and n', and π_i gives the steady-state probability that the i’th state in any perturbed multiplicity is occupied. Simple formulae for the π_i for cascade-type systems derived in C-T&R show that these quantities depend only on the bare-atom radiative decay rates and on the ratio of the Rabi frequencies of the two applied resonant laser beams.

In Sect. 4, the spectral properties of Λ- and V-type dressed-atom gases are considered. It is shown that for these systems, the quantities π_i can only have the values 0, 1, and 1/2 - making analyses of dressed-atom spectra generally much simpler than for cascade-type systems. Because of this simplification, and because dressed-atom lasers in Space would mostly likely involve atoms having V- or Λ-type structures, the focus is mostly placed on these structures in the remainder of the paper. From diagrams analagous to the one used in Sect. 3 to show the allowed spontaneous emission transitions from the perturbed $\varepsilon_{n,n'}$ states of cascade-type atoms, one can determine the fluorescence spectra of Λ- and V-type dressed atoms. In this connection, the Λ-type structure is especially interesting, because *no* fluorescence is emitted by dressed atoms of this type. Utilizing the appropriate dressed-atom spontaneous emission decay diagrams, and recognizing that the π_i values can only be $0, 1$, or $1/2$, one can immediately determine the linear

absorption spectra for both Λ- and V-type dressed atoms in the vicinities of ω_o and ω_o'. For both, absorption occurs in four narrow bands centered at $\omega_o \pm (1/2)\Omega_1$ and $\omega_o' \pm (1/2)\Omega_1$. Although the absorption bands are shifted away from the bare-atom positions, they remain essentially undiminished in strength.

Having acquired basic knowledge about the absorption and fluorescence properties of dressed atoms, one is prepared to inquire how a gas of such atoms would respond to the additional presence of an intense broadband continuum. Both linear and nonlinear optical pumping processes which potentially could provide gain at ω_o and ω_o' in a gas of V-type dressed atoms via absorption of continuum photons are considered in Sect. 5. It is shown that the only optical pumping mechanism capable of explaining the O VI doublet emission intensities observed in symbiotic stars is stimulated hyper-Raman scattering (SHRS), working in conjunction with an equally important process, stimulated hyper-Compton scattering (SHCS), as already noted above.

In Sect. 5, some important results obtained from the scientific literature outlining the difficulties of establishing EIT in three-level systems with large Doppler widths are reviewed. Of most relevance to the possible existence of dressed-atom lasers in Space is the *a priori* deduction one makes from the above mentioned studies that by far the most likely candidates for lasing in such environments would be Λ- or V-type systems having approximately equal bare-atom frequencies. This may help to explain why the O VI emission doublet is so dominant in symbiotic stars.

In Sect. 6, we summarize the principal features of a symbiotic star dressed-atom laser model that represents a synthesis of the main ideas considered in earlier sections of the present paper.

2. The O VI (1032 Å, 1038 Å) doublet emission in symbiotic stars

A symbiotic star is generally considered by astronomers to consist of two stars orbiting together in Space, while remaining a fixed distance apart from one another. One of the stars is assumed to be a decaying red giant, the other an extremely hot white dwarf. The red giant continually loses mass; some of this mass is thought to accrete onto the white dwarf, leading to additional heating of the latter.

Symbiotic star systems are usually divided into two groups: S-type and D-type. These classifications, first made in Webster & Allen 1975, are based on the spectral characteristics of infrared radiation emitted by symbiotic stars in the 1-3 μm region. S-type systems display spectra in this region similar in appearance to the spectra emitted by late-type giants (e.g. M0 III to M5 III). D-type systems have infrared excesses attributable to hot circumstellar dust shells. A typical geometry for an S-type symbiotic star is shown in Fig. 2. Additional astronomical data for RW Hydrae are listed in Schild et al. 1996 as follows: $M_r = 1.6M_\odot$, $M_h = 0.5M_\odot$, $d = 670pc$, and $P \simeq 1$ yr. Here P is the period of the time varying obscuration of the white dwarf by the red giant as seen from Earth. (The plane in which the stars orbit around each other roughly lies in the line-of-sight to RW Hydrae.) D-type systems are more extended binaries than S-type systems, with

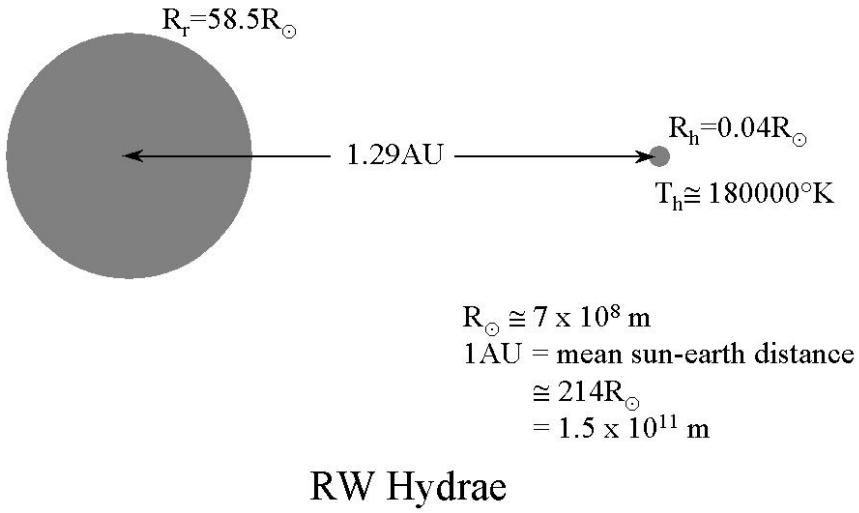

Fig. 2. Sketch of the geometry of the symbiotic star RW Hydrae, based upon measurements presented in Schild et al. (1996).

star separations being more typically 10-20 AU, red giant radii 300-700 $R_\odot$, and orbital periods 16-63 yr.

Much of the enthusiasm that currently exists for symbiotic star research was stimulated by a series of recent spectral studies. Symbiotic stars often show two rather broad emission lines at 6825 Å and 7082 Å Fig.(3). The origins of the two broad red lines, which incidentally are *only* seen in symbiotic stars (although not all such systems - including actually RW Hydrae - have them), remained for about 20 years a mystery in astronomy, until they were finally identified in 1989 by the astronomer H.M. Schmid (Schmid 1989) as spontaneous Raman scattering by ground state hydrogen atoms of light emitted at 1032 Å and 1038 Å on known strong transitions of five-times-ionized oxygen (O VI). These Raman scattering processes are shown in Fig. 4.

The observed ratio of intensities of the 6825-Å and 7082-Å Raman lines is consistent with calculations of the spontaneous Raman scattering cross-sections (Schmid 1989; Sadeghpour & Dalgarno 1992; Lee & Lee 1997). The Raman and Rayleigh cross-sections for excitation by light at 1032 Å and at 1038 Å are given in Lee & Lee 1997 as: $\sigma_{Ram}(1032) = 7.5\ \sigma_T$, $\sigma_{Ray}(1032) = 34\ \sigma_T$, $\sigma_{Ram}\ (1038) = 2.5\ \sigma_T$, $\sigma_{Ray}(1038) = 6.8\ \sigma_T$, where $\sigma_T = 6.6\text{x}10^{-25}$ cm^2 is the Thomson scattering cross-section.

One notes the great differences between the widths of the Raman lines and those of the Ar and He lines in Fig. 3. Schmid et al. 1999 assume the latter emissions to originate in the nebular regions lying between the O VI emission regions and the neutral scattering regions in each of the

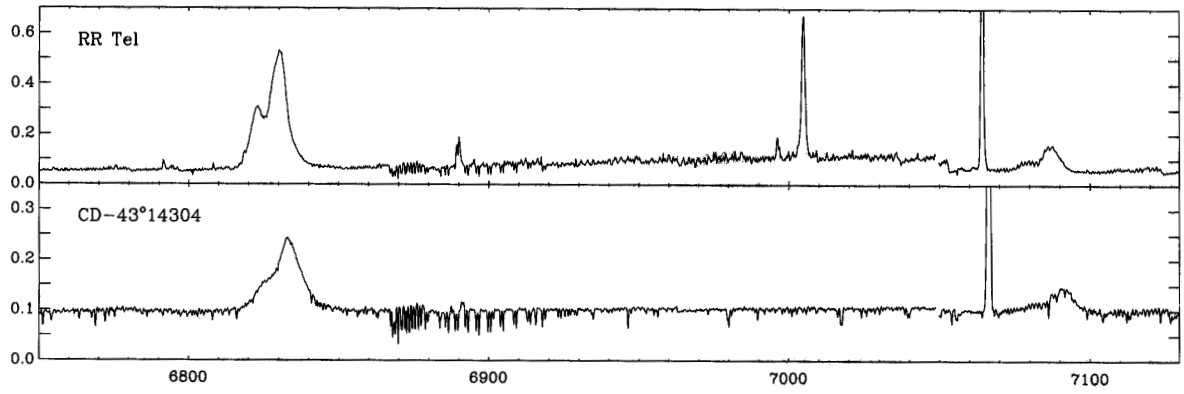

Fig. 3. RR Tel and CD-43°14304 high resolution spectra recorded near the broad Raman scattered O VI lines at ≃6825 Å and ≃7082 Å. The strong, narrow emission lines are due to [Ar V] λ7005 and He I λ7065. Reproduced from Fig. 9 of Schmid et al. (1999).

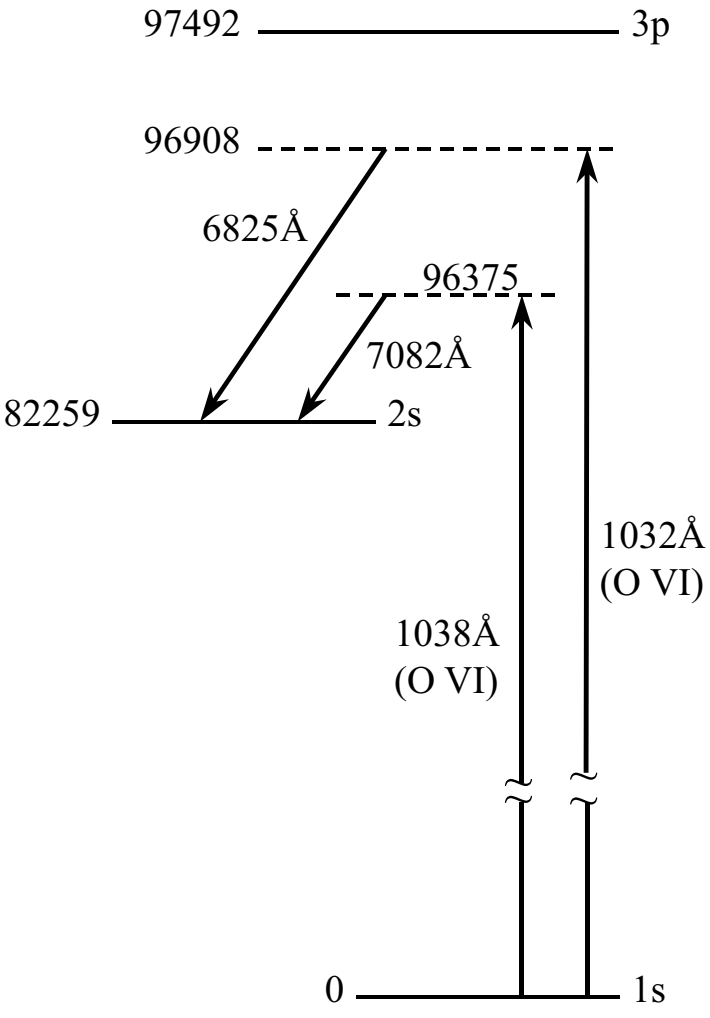

Fig. 4. Spontaneous Raman scattering processes responsible for producing emissions observed at 6825 Å and 7082 Å in symbiotic stars.

model geometries depicted in Fig. 16 of their paper. The sharp He I lines are therefore usually used to determine the radial velocities (RV) of symbiotic star systems. For RR Tel, the system RV value adopted by Schmid et al. 1999 is -62 km s^{-1}. Having determined the system RV values for a number of symbiotic stars, Schmid et al. 1999 then used these values to calibrate the symbiotic star far-UV (FUV) Echelle data they obtained (*vide infra*). In making this calibration, it was assumed that the region of a symbiotic star in which the He I lines are emitted has an RV similar to that for the region in which certain FUV lines (e.g. He II λ1084, O IV] λ1401) are emitted, notwithstanding the fact that the latter would have to originate from within the O VI emission regions in the three scattering geometries shown in Fig. 16 of Schmid et al. 1999.

In the present paper, we focus upon the D-type symbiotic star RR Tel for two main reasons. Firstly, its recorded spectra (both FUV and Raman) possess higher signal-to-noise ratios than those of other symbiotic stars. Secondly, as already mentioned, the plane in which its components orbit happens to be close to the plane of the sky, simplifying somewhat any analysis undertaken.

The Raman lines in symbiotic stars are observed to be polarized. If the region where the O VI doublet emission is generated is assumed to lie fairly close to the hot component, while the spontaneous Raman scattering events are assumed to occur mostly in the red giant atmosphere, it is evident that the polarization angle could then provide the orientation of the symbiotic system binary axis. Such measurements have been extensively performed by astronomers over several years.

Although measurements of the Raman lines alone could provide the basic information needed for the structures of symbiotic stars to be determined, it was only comparatively recently that high quality FUV spectra were obtained for some of these objects. The O VI lines of several symbiotic stars were recorded during the *ORFEUS I* and *ORFEUS II* space shuttle missions STS-51 (September 1993) and STS-80 (November/December 1996). During the first *ORFEUS* mission, the onboard telescope fed the Berkeley spectrometer with resolution 3000. During the second mission, an Echelle spectrometer with resolution 10000 was added. Figures 5- 7 show Berkeley spectra of three symbiotic stars recorded during the first *ORFEUS* space shuttle mission.

One sees from these spectra that the O VI doublet emission indeed completely dominates the FUV spectra of these symbiotic stars over a wide frequency range. These spectra - and those separately obtained with the Hopkins Ultraviolet Telescope during the *Astro*-2 space shuttle mission (Espey et al. 1995) - certainly provided conclusive “smoking gun” evidence for Prof. Schmid’s proposed solution for the mystery of the 6825-Å and 7085-Å lines. As noted in S&G I, viewing these remarkable spectra left us with the intuitive feeling that laser action of some kind must be going on in symbiotic star systems, and we then proceeded to construct and analyze the two-level-atom space laser model that became the basis of that paper. As explained in the Introduction, one of the main aims of the present paper is to show that the three-level-atom space laser model can more realistically account for symbiotic star spectral data than can the two-level-atom model.

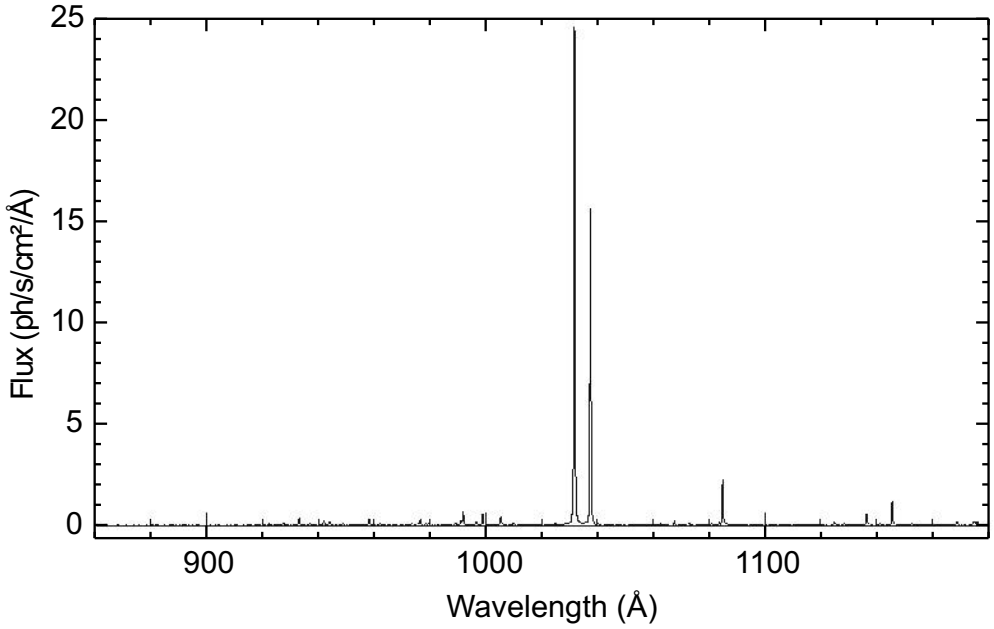

Fig. 5. Spectrum of RR Tel from the *ORFEUS I* spectral data browser. (http://albert.ssl.berkeley.edu/orfeus/spec-list-rr_tel.html)

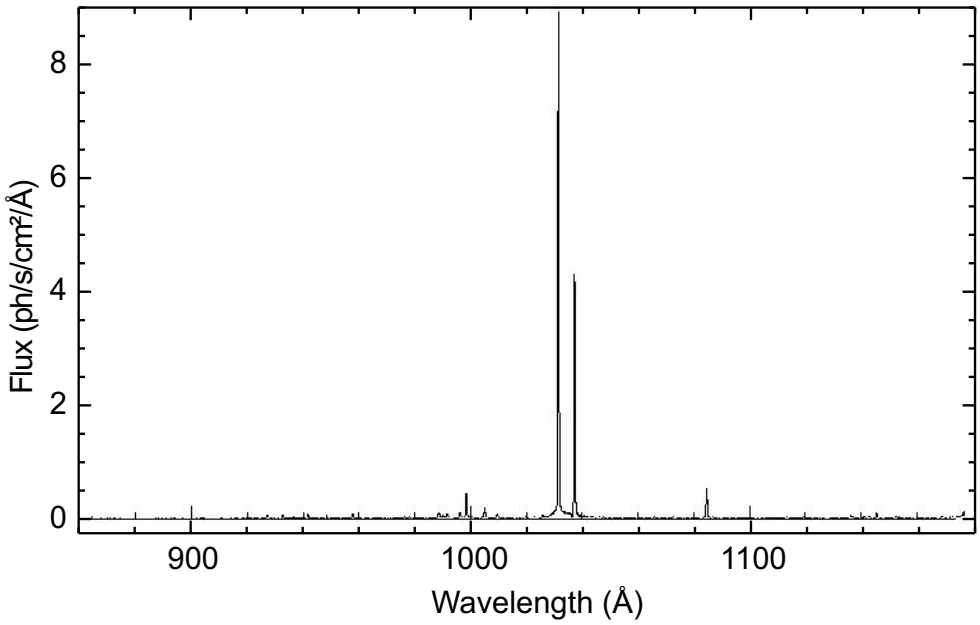

Fig. 6. Spectrum of AG Dra from the *ORFEUS I* spectral data browser. (http://albert.ssl.berkeley.edu/orfeus/spec-list-ag_dra.html)

From Figs. 5- 7, one notes that the doublet emission intensity ratio varies greatly from symbiotic star to symbiotic star - from about 10:1 in Z Andromeda, to about 2.3 in AG Draconis, to about 1.7 in RR Telescopii. In S&G I, it was suggested that such observed widely varying intensity ratios should present a formidable difficulty for the basic explanation astronomers have long offered to explain the superintense O VI doublet emission in symbiotic stars. According to

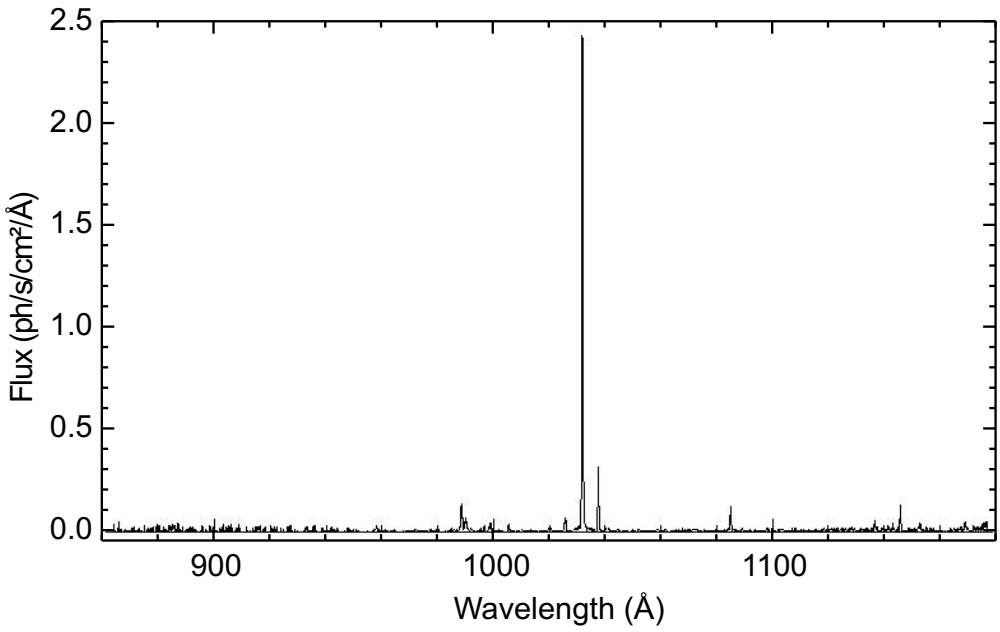

Fig. 7. Spectrum of Z And from the *ORFEUS I* spectral data browser. (http://albert.ssl.berkeley.edu/orfeus/spec-list-z_and.html)

the standard model, this emission occurs either through recombination of O VII ions with electrons, or from electron impact with O VI ions. With both mechanisms, one theoretically expects a doublet emission intensity ratio of 2:1, whereas the actual values that have been observed in symbiotic stars vary over a range from ≈10:1 to ≈1:1. However, in preparing the manuscript for S&G I, we were unaware that a convincing explanation for *large* (*i.e.* >2) observed values of this ratio had already been given in Schmid et al. 1999. It was shown in that work that clustered in wavelength about the 1038-Å O VI line are the five strongest B5-0 absorptions of H_2, as well as strong atomic absorptions from C II $\lambda\lambda$1036.34, 1037.02 and O I λ1039.23. Interstellar absorption by these species present in the line-of-sight to a symbiotic star can completely account for large observed values of the doublet intensity ratio, since there exist no strong atomic or H_2 absorption lines with wavelengths in the vicinity of the O VI 1032-Å line. Of the three symbiotic stars shown in Figs. 5- 7, RR Tel is observed to have the smallest value (1.7) for the O VI doublet intensity ratio. This is expected, since this object is located at high galactic latitudes. However, no explanation has yet been given to account for the fact that this value is actually <2. In the case of CD-43°14304, the O VI doublet intensity ratio is observed to be even lower, 1.4 (Schmid et al. 1999). Both low and high values of the O VI doublet emission intensity ratio could occur on the basis of the dressed-atom space laser model that is here being proposed.

Figure 8 shows high-resolution Echelle spectra of the O VI FUV doublet emission in four symbiotic stars. From these, one sees that the doublet emission components have true spectral widths on the order of 20-30 wavenumbers (FWHM).

Several models for Raman scattering in symbiotic stars have been published (e.g. Schmid 1996, Lee & Lee 1997, Harries & Howarth 1997). In each of these papers, a Monte Carlo method

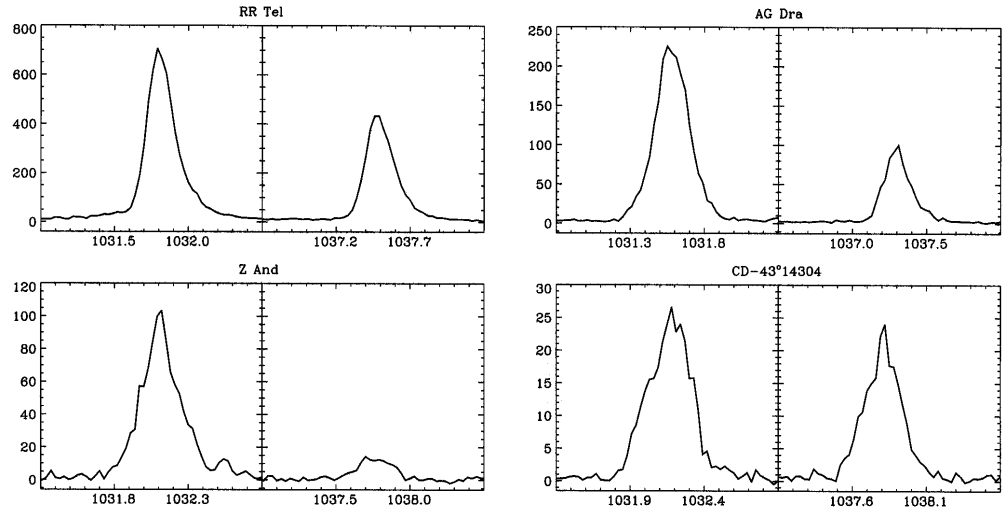

Fig. 8. *ORFEUS II* Echelle spectrograph line profiles for O VI doublets in RR Tel, AG Dra, Z And, and CD-43°14304. Reproduced from Fig. 2 of Schmid et al. (1999).

was used to calculate the profiles and polarizations of Raman scattered O VI lines in symbiotic stars. It is beyond the scope of the present paper to summarize this extensive work. No discussion of polarized Raman spectra will here be presented, even though such measurements potentially carry more information about the structures of symbiotic stars than do Raman intensity spectra. We here will only consider the double-peaked 6825-Å Raman intensity spectrum in RR Tel (Fig. 3). We will attempt to interpret the profile of this band utilizing a model in which a dressed-atom laser is substituted for the parent FUV source in the symbiotic star structure assumed in Harries & Howarth 1997 (hereafter denoted by H&H 1997).

The model of H&H 1997 consists of a giant star, radius R_r, and an isotropically emitting point source of O VI photons, separated from the red giant by a distance $R_r q_{sep}$. (The effects of an extended O VI source were also explored in H&H 1997, but were basically found only to reduce the intensity of the polarized-flux spectra.) The giant star has an extended atmosphere, which is assumed to be spherically symmetric. For a mass-losing star, the H-atom density $\rho(r)$ is determined by both the stellar mass-loss rate $\dot{M}_r$ and velocity $v(r)$ through the equation of mass conservation:

$$\rho(r) = \dot{M}_r / 4\pi r^2 v(r). \qquad (3)$$

In most other symbiotic star Raman scattering models, a spherically symmetrical red giant wind is also assumed. None of the models considers the possibility that the mechanism usually invoked to explain mass transfer in binary systems that strongly emit X-rays - i.e. Roche-lobe overflow with formation of an accretion disk about the hot star - applies in the case of symbiotic stars. Evidently, the star separation is too great in the latter systems for this mechanism to work. This would hold especially true for D-type symbiotic stars.

In H&H 1997, a benchmark reference model is first created, and then the effects of changing the free parameters of that model are studied. For the reference model, the following parameter

values were adopted: $\dot{M}_r = 10^{-6} M_\odot$ yr^{-1}, $R_r = 100\ R_\odot$, $M_r = \sim M_\odot$, a mass ratio of the two stars ~1, and a binary period P of ~1 year. These values imply that the binary separation factor q_{sep} is ~5. The benchmark model parameters here assumed are seen to be ones that are appropriate for S-type symbiotic star systems. However, in H&H 1997 it is noted that the overall scattering geometry is unaffected by simple scalings; that is, the results would be similar for models which have the same values of both q_{sep} and $\dot{M}_r\ /R_r$.

For their reference model, H&H 1997 adopt a constant-velocity outflow, with $v(r) = v_\infty =$ 50 km s^{-1}. H&H 1997 note that, with such a relatively high outflow speed, the velocity structure in the Raman lines is more clearly revealed. In a constant-velocity-wind model, there is a finite H-atom density at the wind base (i.e. at the red-giant surface). From Eq. (3), one determines that in the H&H 1997 reference model this density is about 1.2 x 10^{10} H atoms cm^{-3}. There thus exists the possibility that a parent FUV photon can reach the red-giant surface without scattering. To treat this case, H&H 1997 adopt for their reference model a “core-halo” geometry consisting of an extended wind and a thin, static photosphere.

Figure 9 shows an example of calculations performed in H&H 1997 to demonstrate the effect of changing various parameter values in their reference model. Here 6825-Å Raman-line polarization spectra are plotted for the reference model viewed at quadrature, with the red giant mass-loss rate being the parameter that is varied. Most of the calculated plots shown in Fig. 9 are seen to involve polarized Raman scattering features. These are fully explained in H&H 1997. As stated earlier, in the present paper we are basically interested in explaining Raman Stokes intensity spectra, which in Fig. 9 are shown in the bottom row. The spectral structures are better resolved in the polarization spectra, and H&H 1997 make use of this fact to aid them in determining the correspondence between the various peaks in Fig. 9 and the spatial regions of the symbiotic star in which the Raman scatterings that produce the peaks occur.

H&H 1997 interpret part of the spectral structure seen in Fig. 9 as follows: “The intensity profile of the log $\dot{M}$ = -7 model shows a two-peaked intensity structure, with the bluewards peak centred at the Raman-line rest wavelength, showing that it is a result of photospheric scattering. The polarized flux is triple-peaked, with all the peaks polarized in the same direction; there is no polarization flip. The three peaks originate in the material between the two stars (approaching the O VI source), in the red giant photosphere, and in the region ’behind’ the red giant (as seen from the hot component). There is, relatively speaking, insufficient material ‘above’ and ‘below’ the hot component to introduce significant features at orthogonal polarizations. This interpretation is confirmed by the log $\dot{M}$ = -8 model, which shows a two-peaked intensity profile, with the bluewards peak the strongest. This peak corresponds to photospheric scattering; there is very little scattering in the rarified wind. The polarized flux peak again occurs at the Raman-line rest wavelength, and is a result of photospheric scattering. The very small redward peak is associated with wind scattering in the extended region ‘behind’ the red giant.”

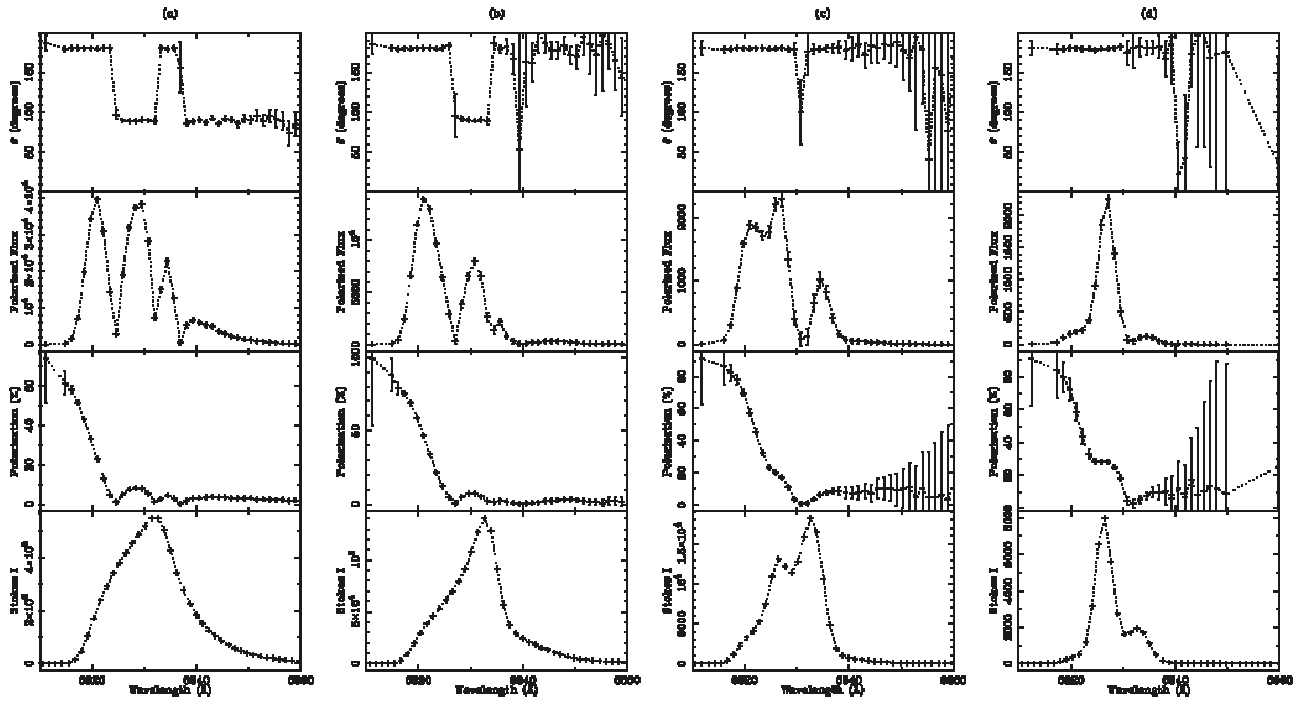

Fig. 9. Calculated 6825-Å Raman-line polarization spectra for the reference model of Harries & Howarth (1997) viewed at quadrature, with the red giant mass-loss rate being the parameter that is varied. Reproduced from Fig. 13 of Harries & Howarth (1997).

Figure 9 demonstrates that the mass-loss rate (or, more importantly, the H-atom density distribution) has a dramatic effect on both the Raman-line intensity and polarization structures. Consideration of all the scattering scenarios represented in this figure leads to the following simple interpretation of the RR Tel 6825-Å Raman profile in Fig. 3 on the basis of a dressed-atom laser model.

As in the reference model of H&H 1997, a spherically-symmetric red giant wind with constant wind velocity v is assumed. It is further assumed that all species of atoms (e.g. H, O, etc.) of this wind move with the same velocity. As O atoms in this wind approach the hot star, they become photoionized by the hot star continuum, and the ions (e.g. O VI) which result continue to move in the same direction with the same velocity v. The two frequency components of a dressed-atom laser beam proceeding from hot star to cool star would both be Doppler-downshifted by the motion of the incoming O VI ions. In the rest frame of the symbiotic star, the frequency of the shorter wavelength component would be $\nu_{1032} - \nu_{1032}v/(3 \text{ x } 10^8)$. For ν_{1032} we adopt the value listed in Moore 1971 (96907.5 cm^{-1}).

If the longer wavelength component of the RR Tel 6825-Å band in Fig. 3 is attributed to light produced by Raman scattering of dressed-atom laser beam photons in the red giant photosphere, one can then determine what the value of the velocity v must be. On the basis of Fig. 3 (and also Fig. 15 of Schmid et al. 1999), it appears that from Earth one observes the center of the redward peak of the 6825-Å RR Tel band to fall approximately at an air wavelength of 6829.0 Å. Using the formula $\nu_{vac} = 0.999724/\lambda_{air}$ (cm^{-1}) to convert wavenumbers in vacuum to wavelengths in air

(e.g. as in Jenniskens & Désert 1994), one finds the equivalent vacuum wavenumber frequency to be 14639.39 cm^{-1}. With use of the same RR Tel system RV value (-62 km s^{-1}) adopted in Schmid et al. 1999, this transforms to a Raman frequency of 14636.37 cm^{-1} in the rest frame of the symbiotic star. Since there is no relative motion between the red giant photosphere and the hot star, this implies that the dressed-atom laser frequency in the symbiotic star rest frame is 14636.37 + 82258.94 (H 2s level energy listed in Moore 1971) = 96895.3 cm^{-1}, which is downshifted by 12.2 cm^{-1} from ν_{1032}. The value of v that would produce this amount of downshifting is v = 37.8 km s^{-1}, reasonably close to the value 50 km s^{-1} assumed in the reference model of H&H 1997. Viewed from Earth, the dressed-atom laser frequency would be 96895.3 + (96895.3)(62 x 10^3)/(3 x 10^8) = 96915.32 cm^{-1} (≡1031.83 Å). This wavelength is seen to be reasonably close to the wavelength at which the 1032-Å doublet component of RR Tel peaks in Fig. 8.

Raman scattering of ≃1032-Å dressed-atom laser photons by H atoms moving in the wind from red giant to hot star would produce Stokes photons with a frequency in the rest frame of the symbiotic star equal to [ν_{1032} - $\nu_{1032}v$/(3 x 10^8)] - [82258.94 - (82258.94) v /(3 x 10^8)]. For v = 37.8 km s^{-1}, one finds this Stokes frequency to be 14646.71 cm^{-1}. The frequency of the Raman scattered light viewed from Earth would thus be 14646.71 + (14646.71)(62 x 10^3)/ (3 x 10^8) = 14649.74 (vacuum) cm^{-1}. This is equivalent to an air wavelength of 6824.2 Å - about one Angstrom longer than the blueward peak of the 6825-Å RR Tel Raman band in Fig. 3, but nevertheless in reasonable agreement with it.

On the basis of the calculations shown in Fig. 9, assignment of the two peaks of the RR Tel 6825-Å emission band in Fig. 3 to Raman scattering of dressed-atom-laser photons by H atoms located in the wind moving between the stars and in the red giant photosphere would qualitatively suggest that in this symbiotic star system the mass-loss rate must correspond most closely to the value assumed in column (c) of Fig. 9. In the case of RR Tel, there is no Raman intensity band that corresponds to the longest wavelength band shown in Fig. 9c. The latter represents scattering by H atoms located “behind” the red giant. Presumably, in RR Tel, the relatively small angle of divergence θ of the dressed-atom laser beam causes it to be “blocked” by the red giant photosphere. In RR Tel, there is also no observed intensity band corresponding to a polarization flip of 90° . Such a band would be produced via Raman scattering of parent FUV photons by H atoms located “above” and “below” the hot white dwarf. In the dressed-atom-laser model, one would not expect the generated field to extend significantly into these regions.

It is necessary to explain how strong emissions at 1032 Å and 1038 Å in RR Tel are seen from Earth, since it is assumed in the model that the dressed-atom laser beam is confined to a comparatively narrow region between the two stars (Fig. 10). There are three possible contributing sources for this emission: (1) fluorescence of O VI ions excited via the SHRS laser pumping process, (2) Rayleigh scattering of dressed-atom laser beam photons by H atoms in the red giant wind, and (3) fluorescence that must be emitted from a gas of V-type dressed atoms irradiated strongly enough by monochromatic light at the two resonance frequencies that the “secular approximation“ (Sects. 3, 4) applies. We initially discuss the first mechanism.

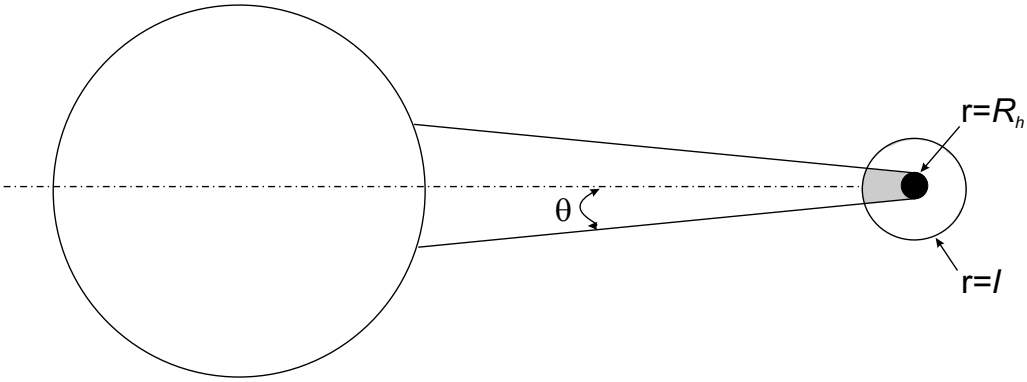

Fig. 10. Schematic diagram showing postulated geometry of a dressed-atom laser beam in a symbiotic star. The continuous-wave (CW) laser beam originates at the hot star surface and propagates along the symbiotic star axis towards the red giant. All amplification of the laser beam occurs in the cross-hatched region. Within a spherical region of radius l about the hot star, all atoms in the red giant solar wind are assumed to be ionized.

As explained in Sect. 5, generation of every O VI laser photon through the SHRS process is simultaneously accompanied by the absorption of two photons from the thermal continuum and the excitation of an O VI ion to one of the two upper electronic states. The ions which have been electronically excited in this way immediately fluoresce, and this fluorescence is seen from Earth as intense emission at 1032 Å and 1038 Å. Strictly speaking, there is a somewhat subtle point to be considered here. For simplicity, we continue to consider the symbiotic star to be viewed from Earth in quadrature (Fig. 10). In the rest frame of this system, fluorescence emitted in the direction of the Earth would occur at the normal O VI transition frequencies, ν_{1032} = 96907.5 cm^{-1} and ν_{1038} = 96375.0 cm^{-1}, not at the dressed-atom laser frequencies, which are Doppler downshifted by the motion of O VI ions in the red giant wind. The presence of a dressed-atom laser beam implies that a condition of EIT has been established in the O VI ion gas in the region occupied by the beam (cross-hatched region in Fig. 10). In this gas, therefore, there will exist two spectral intervals of complete transparency, each centered about one of the two dressed-atom laser frequencies. Replacing the two O VI ion linear absorption bands originally present in the two spectral intervals made transparent by EIT are four new “dressed-atom“ absorption bands, equally offset to both sides of each dressed-atom laser frequency (Sects. 3, 4, and Fig. 10 of S&G I). O VI fluorescent photons generated via SHRS pumping and propagating in a direction towards Earth will be nearly resonant with two of these new absorption bands, and will therefore at once undergo elastic scattering. As a result of this scattering, the fluorescent photons cannot immediately escape from the region occupied by both O VI ions and the laser beam. Subsequent elastic scatterings then occur. After many such scatterings, the fluorescent photon frequencies will become shifted into the spectral regions of transparency, and the photons will then escape from the symbiotic star. Thus the O VI fluorescence that is induced by the SHRS process will be seen from Earth to occur at the dressed-atom laser frequencies. The spectral extent of fluorescent light emitted by O VI ions excited via the SHRS pumping process will be proportional to the

square root of the average dressed-atom laser intensity in the region where the fluorescence is emitted (Sects. 3, 4). Thus the inherent fluorescence linewidth should in principle increase with increasing distance from the hot star. However, the elastic scatterings that the fluorescent photons undergo before they escape from the symbiotic star will also contribute to broadening of the fluorescent lines.

In seeking to calibrate roughly the intensity of the hidden dressed-atom laser beam from the observed intensity of fluorescence, it is helpful to consider a still more simplified version of the model shown in Fig. 10, one in which the hot star in RR Tel is represented by a cube of edge dimension h, centered at the star and oriented with four surfaces parallel to the symbiotic star axis. The dressed-atom laser beam, of cross-sectional area h^2, is now assumed to originate at the surface of the cube facing the cool star, and to propagate without divergence along the symbiotic star axis towards the latter, becoming fully amplified in a pathlength l, where l is much less than the distance between the stars, but much greater than h. Here l can be interpreted as the radius of a spherical region about the hot star in which all the O VI ions are contained.

In this ultrasimplified model, the number of fluorescent photons per second emerging from one lxh face of the rectangular volume occupied by the laser beam should roughly correspond to one-quarter the number of photons per second in the beam leaving the rectangular volume through the hxh surface at $r = l$. In principle, it should therefore be possible to estimate the power of the hidden dressed-atom laser beam by comparing the observed fluorescence intensity with the thermal continuum level intensity. The latter can be roughly approximated as follows.

In S&G I, an estimate was made of the thermal continuum intensity that should exist in symbiotic stars, based upon use of the standard photon distribution law giving the emittance of photons per cm^2 per second from the surface of a hot body at a given temperature. For a star temperature of 180000°K, the continuum intensity at 1000 Å at the star surface is about 16W/cm^2 in a 160-MHz bandwidth. This is about 3 kW/cm^2 in a one-wavenumber-wide bandwidth, or about 100 kW/cm^2 in a 33-wavenumbers-wide bandwidth. This last number is of especial interest for the following reason. The spectral resolution of the Berkeley spectrometer used to take symbiotic star spectra during both *ORFEUS* missions was about 3000. This implies that each detector element (i.e. “bin”) tallied all incident photons with frequencies falling within the ~33-wavenumbers-wide spectral range monitored by the bin. For all bins, the incident photons included those representing continuum light emitted by the hot white dwarf. Hence the observed thermal continuum background levels surrounding the O VI doublet emissions in symbiotic star spectra recorded with the Berkeley spectrometer should correspond to blackbody continuum intensities emitted near the hot star of roughly 100 kW/cm^2. Figure 11 shows the spectrum of RR Tel at very high gain. One can clearly see the continuum level here, with an average value of about 0.04 in the units shown. The continuum appears mostly flat throughout the spectral region shown. The continuum appears cut off at wavelengths shorter than 912 Å, and this is due to the presence of H atoms distributed in interstellar space along the line-of-sight to RR Tel. In the on-scale spectrum of RR Tel (Fig. 5), the flux at the peak of the 1032-Å line is about 24 in the

same units. Therefore, in RR Tel the peak intensity of the strongest doublet component exceeds the continuum level by approximately a factor 600. On the basis of the crude simplified model discussed above, in which the hot star continuum photons that are detected from Earth would all pass through the *hxh* cube surface that faces the Earth, one deduces that the intensity of the non-diverging 1032-Å dressed-atom laser beam at $r = l$ would be about 240 MW/cm^2. From this, one would conclude that the SHRS photonic mechanism which pumps the dressed-atom laser must be able to facilitate efficient conversion of thermal continuum photons in a spectral range extending more than ~80000 cm^{-1} on either side of the O VI FUV lines into narrow-band emission at ≃1032 Å. This number does seem excessively large, especially since only the power budget for the 1032-Å doublet component is here being considered. Taking into account the possibility that some of the observed RR Tel FUV emission represents Rayleigh scattering of dressed-atom laser photons by H atoms in the red giant wind helps to reduce this number somewhat. For example, if 80% of the 1032-Å dressed-atom laser photons present in the beam at $r = l$ are subsequently elastically scattered by H atoms in the symbiotic star (i.e. leaving 20% to be Raman scattered), power for the 1032-Å laser beam could theoretically be provided via total conversion of continuum photons existing in a spectral range extending ≃44000 cm^{-1} on either side of the O VI FUV resonance doublet. The power in the laser beam at $r = l$ would then be ~133 MW/cm^2. A third source potentially contributing to the observed FUV emission from a symbiotic star was listed earlier to be the fluorescence inherently emitted by a strongly driven V-type dressed-atom gas (Sect. 4). An upper limit to this contribution can be roughly estimated by considering the fluorescence that would be emitted from a column (length l) of excited O VI ions, taking the excited state density to be the value of the total O VI ion density in the red giant wind near the hot star. For an O VI ion density = 10^4 cm^{-3} (the value used in S&G I in estimating the unsaturated two-level-laser gain induced by SHRS), a fluorescence lifetime of 1 nanosecond, and a column length $l = 0.8\ R_\odot$, the fluorescence power radiated in all directions via this mechanism from a column of length l and cross-sectional area of unity would be no more than ~1.2 MW, which is seen to be negligible compared to the contributions of the other two sources.

All told, the overall very high O VI FUV doublet emission intensities that are inferred to occur in RR Tel from the above rough estimates impose an enormous requirement on any viable pumping mechanism, which leads to the strong conclusion to be made in Sect. 5 that SHRS acting alone cannot generate such high narrow-band laser power, and that a concomitantly occurring supplementary nonlinear process, stimulated hyper-Compton scattering (SHCS), must also be operative in symbiotic star systems.

As stated earlier, the standard explanation for the intense O VI FUV doublet emission in symbiotic stars is based upon a photoionization model. In this connection, it is perhaps worth noting that a substantial attempt was made in Espey et al. 1995 to utilize such a model to account quantitatively for the relative intensities of the RR Tel FUV emission lines observed in the same work. The photoionization model employed by these authors utilized the CLOUDY code (Ferland 1993) to predict the spectrum of a constant-density cloud illuminated by the RR

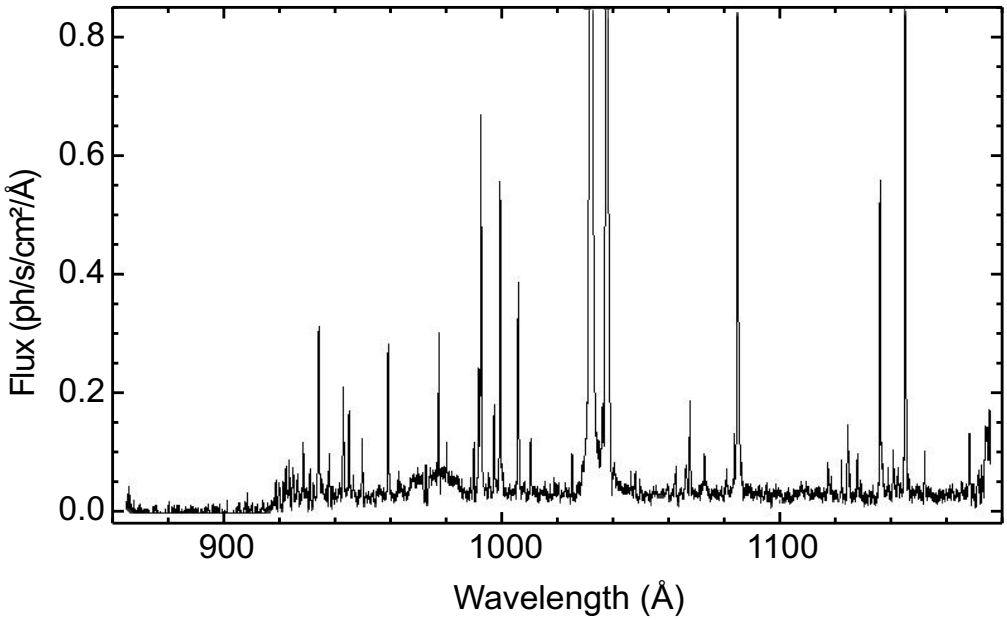

Fig. 11. Spectrum of RR Tel (shown at high gain) from the *ORFEUS I* spectral data browser. (http://albert.ssl.berkeley.edu/orfeus/spec-list-rr_tel.html)

Tel ionizing spectrum. However, the calculated relative emission intensities of the O VI doublet were found by Espey et al. 1995 to be very much lower than the observed values. For example, the intensity ratio of the λ1035 O VI doublet emission to the λ1549 C IV doublet emission was measured to be about 3.2, yet the predicted ratio was only 0.049. Regarding this, and other such discrepancies, Espey et al. 1995 simply conclude: “... It is apparent that a more complex model of the RR Tel system is necessary, ...”.

Figure 12 shows the incredibly simple energy level diagram of O VI ions. The two transitions corresponding to the O VI FUV doublet emissions are fully allowed, and the one between the $^2P_{3/2}$ and $^2P_{1/2}$ levels is basically unallowed. Since the next highest O VI energy level is at 640000 cm $^{-1}$, the three levels shown in Fig. 12 can be conceptually isolated from all other O VI levels. This, together with the fact that no hyperfine splitting exists in any of the levels, since the mass number of the O^{16} isotope (99.76% abundant) is even and the nuclear spin is therefore 0, allows one to regard the O VI ion as having an ideal V-type, three-level-atom, structure. As was explained in S&G I, with an energy level diagram as simple as this, it would be virtually impossible for normal laser action to occur. Normal lasing occurs on transitions that are inverted, that is, on ones that have more atoms maintained in the upper than in the lower state, so that stimulated emission can exceed stimulated absorption. Here there are no higher levels which might somehow be pumped, with excited ions then dropping into the upper levels of the O VI doublet transitions. It was therefore strongly inferred in S&G I that some unusual pumping mechanism must be operative here. As already mentioned above several times, it will be argued in Sect. 5 that a combination of two processes, stimulated hyper-Raman scattering (SHRS) and

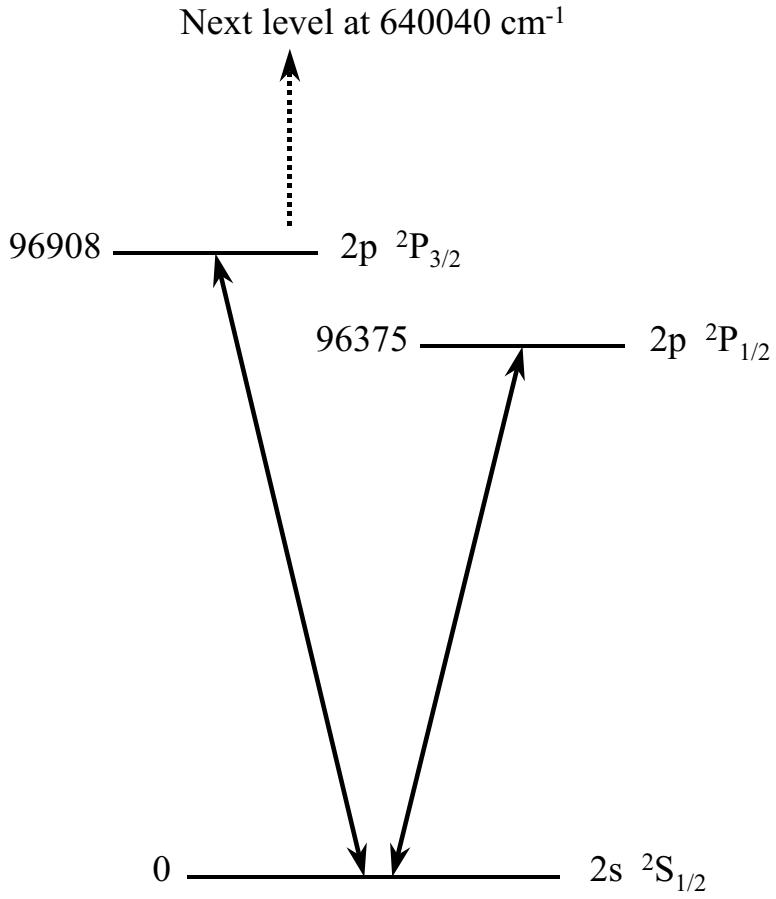

Fig. 12. Energy level diagram for the O VI ion.

stimulated hyper-Compton scattering (SHCS), occurring about *both* bare-atom transitions in a dressed-atom O VI gas, is the only photonic pumping scenario with which one can plausibly account for the efficient conversion of extremely broad spectral ranges of incoherent continuum light into narrow-band laser light.

3. Fluorescence and absorption spectra of cascade-type dressed atoms

An energy level diagram similar to the one with which C-T&R introduce the concept of unperturbed, threefold-degenerate multiplicities $\varepsilon_{n,n'}$ is shown in Fig. 13. Wavy arrows pointing to the left or to the right describe the emission of a fluorescence photon on transitions *ab* or *bc*, respectively.

For cascade-type three-level atoms, Fig. 14 shows the unperturbed degenerate states of the multiplicity $\varepsilon_{n,n'}$ and indicates the couplings that are induced between these states by the presence of the two resonant light fields. The matrix element for the interaction Hamiltonian $\mathcal{H}_{int}$ that couples together two states of a multiplicity - for example, $\mid a, n+1, n' \rangle$ and $\mid b, n, n' \rangle$ - can generally be written as (see Cohen-Tannoudji et al. 1992, p.415)

$$\langle b, n, n' \mid \mathcal{H}_{int} \mid a, n+1, n' \rangle = -\frac{1}{2}\mu E(\omega_o) = \frac{1}{2}\hbar\omega_1 \qquad (4)$$

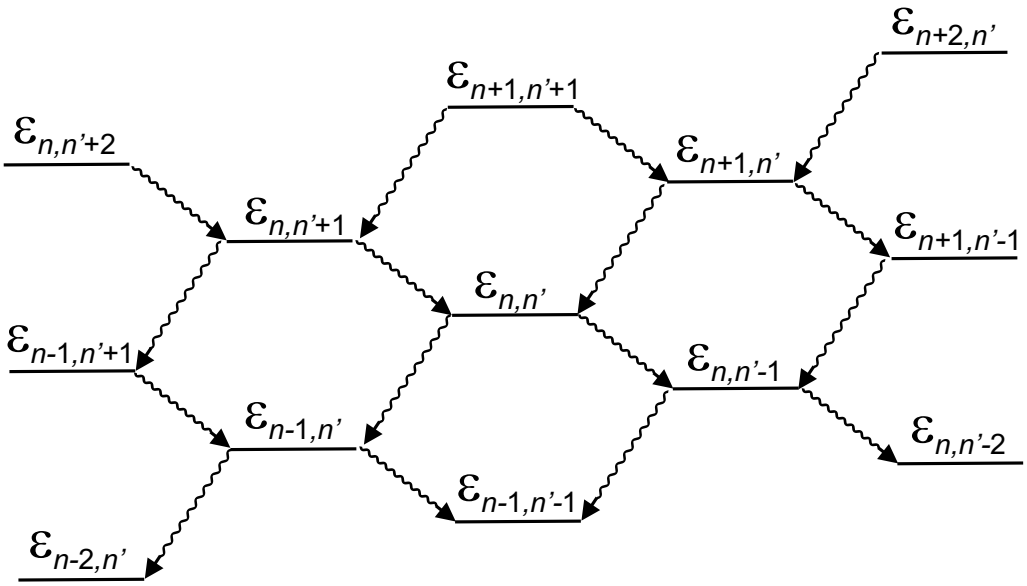

Fig. 13. Energy level diagram showing some of the (three-fold degenerate) unperturbed multiplicities $\varepsilon_{n,n'}$. Wavy arrows pointing to the left or to the right depict the emission of a fluorescence photon on transitions *ab* or *bc*, respectively. After Fig. 3 of Cohen-Tannoudji & Reynaud (1977).

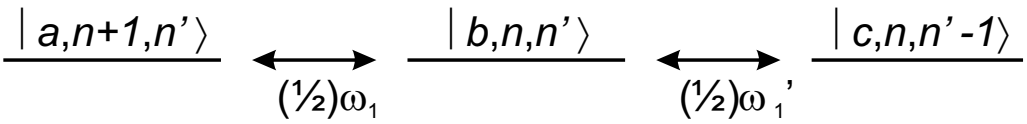

Fig. 14. Unperturbed degenerate states of the multiplicity $\varepsilon_{n,n'}$ for cascade-type three-level atoms. The double-headed arrows represent the couplings between the degenerate states, proportional to the Rabi frequencies ω_1 and ω_1'. After Fig. 4 of Cohen-Tannoudji & Reynaud (1977).

where μ is the *ab* transition dipole moment, $E(\omega_o)$ is the maximum value of the sinusoidally-varying electric field of the light beam at ω_o, and Ω_1 is the Rabi frequency for this beam. (In the shorthand notation used in C-T&R, the quantity $\hbar$ appearing in Eq. (4) is taken to be equal to 1, as already mentioned.)

Diagonalization of the couplings inside each multiplicity $\varepsilon_{n,n'}$ is performed by C-T&R in the following manner. Two linear combinations of $|\ a, n+1, n'\rangle$ and $|\ c, n, n'-1\rangle$ are introduced which are respectively coupled and uncoupled to $|\ b, n, n'\rangle$. One first defines a “generalized Rabi frequency” Ω_1 in terms of the individual Rabi frequencies ω_1 and ω_1' of the two resonant laser beams.

$$\Omega_1 = \left(\omega_1^2 + \omega_1'^2\right)^{1/2} \tag{5}$$

Defining an angle α by

$$tan\alpha = \omega_1'/\omega_1 \tag{6}$$

one then writes

$$|\ u, n, n'\rangle = \cos\alpha\ |\ a, n+1, n'\rangle + \sin\alpha\ |\ c, n, n'-1\rangle \tag{7}$$

and

$$| v, n, n' \rangle = -\sin\alpha \,|\, a, n+1, n' \rangle + \cos\alpha \,|\, c, n, n'-1 \rangle \tag{8}$$

Using Eq. (4), one readily verifies that $| v, n, n' \rangle$ is not coupled to $| b, n, n' \rangle$, while $| u, n, n' \rangle$ is coupled to this state with an amplitude $(1/2)\Omega_1$. C-T&R thus deduce that $\varepsilon_{n,n'}$ splits into three perturbed states $| i, n, n' \rangle$ $(i = 1, 2, 3)$

$$\begin{aligned} | 1, n, n' \rangle &= \frac{1}{\sqrt{2}} (| b, n, n' \rangle + | u, n, n' \rangle) \\ | 2, n, n' \rangle &= | v, n, n' \rangle \\ | 3, n, n' \rangle &= \frac{1}{\sqrt{2}} (-| b, n, n' \rangle + | u, n, n' \rangle) \end{aligned} \tag{9}$$

with energies (measured with respect to the unperturbed energy of $\varepsilon_{n,n'}$) respectively equal to:

$$\begin{aligned} E_1 &= +\frac{1}{2}\Omega_1 \\ E_2 &= 0 \\ E_3 &= -\frac{1}{2}\Omega_1 \end{aligned} \tag{10}$$

These perturbed levels are shown in Fig. 15. Using Eqs. (7, 8, 9), one can finally write the dressed-atom wavefunctions as linear combinations of the bare-atom wavefunctions for the cascade-type structure:

$$\begin{aligned} | 1, n, n' \rangle &= \frac{1}{\sqrt{2}} (\cos\alpha \,|\, a, n+1, n' \rangle + | b, n, n' \rangle) \\ &\quad + \frac{1}{\sqrt{2}} (\sin\alpha \,|\, c, n, n'-1 \rangle) \\ | 2, n, n' \rangle &= -\sin\alpha \,|\, a, n+1, n' \rangle + \cos\alpha \,|\, c, n, n'-1 \rangle \\ | 3, n, n' \rangle &= \frac{1}{\sqrt{2}} (\cos\alpha \,|\, a, n+1, n' \rangle - | b, n, n' \rangle) \\ &\quad + \frac{1}{\sqrt{2}} (\sin\alpha \,|\, c, n, n'-1 \rangle) \end{aligned} \tag{11}$$

As a consequence of the assumption that the *ac* transition is forbidden, the only non-zero matrix elements of the atomic dipole moment operator **M** are $\mu = \langle a \mid \mathbf{M} \mid b \rangle$ and $\mu' = \langle b \mid \mathbf{M} \mid c \rangle$. Utilizing this fact, and making use of the wavefunction expansions appearing in Eqs. (11), one can easily evaluate the dipole moment matrix elements for all allowed spontaneous emission decays originating from each of the three perturbed levels$| i, n, n' \rangle$ of a given multiplicity $\varepsilon_{n,n'}$ and terminating on the various perturbed levels of lower-lying multiplicities. (It becomes at once apparent that **M** couples $\varepsilon_{n,n'}$ only to adjacent multiplicities ($\varepsilon_{n\pm1,n'}$ or $\varepsilon_{n,n'\pm1}$).) Equation (2.12) of C-T&R displays these dipole moment matrix elements in the form of two simple tables. The individual dipole moment matrix elements are either zero, or are equal to μ or μ' multiplied by simple factors such as $(1/2)\cos\alpha$, $-(1/\sqrt{2})\sin\alpha$, etc. The individual spontaneous emission decay rates, obtained by squaring the various dipole matrix elements, are again either zero, or are equal

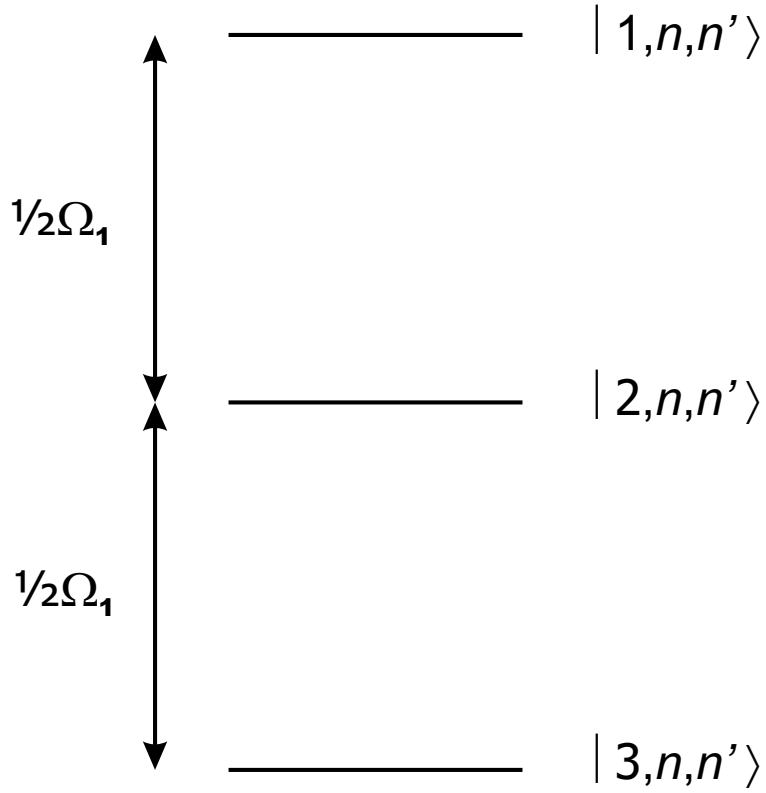

Fig. 15. Perturbed states of the multiplicity $\varepsilon_{n,n'}$, with a splitting determined by the generalized Rabi frequency $\Omega_1 = (\omega_1^2 + \omega_1'^2)^{1/2}$. After Fig. 5 of Cohen-Tannoudji & Reynaud (1977).

to γ or γ' multiplied by simple factors such as (1/4) $\cos^2 \alpha$, (1/2) $\sin^2 \alpha$, etc. Here γ and γ' are the fluorescence decay rates of the two bare-atom transitions $b \rightarrow a$ and $c \rightarrow b$.

For three-level cascade-type atoms, the allowed spontaneous emission decays from the three perturbed states of $\varepsilon_{n,n'}$ are shown as wavy arrows in Fig. 16. One instantly sees that the fluorescence spectrum $F_{ab}(\omega)$ observed on the transition $b \rightarrow a$ has five components at frequencies ω_o, $\omega_o \pm (1/2)\Omega_1$, and $\omega_o \pm \Omega_1$. A similar result holds for $F_{bc}(\omega)$, which exhibits five components at ω_o', $\omega_o' \pm (1/2)\,\Omega_1$, and $\omega_o' \pm \Omega_1$. The widths and the weights of the various components are evaluated in C-T&R. The widths of the lateral components about both ω_o and ω_o' are the same, and are given by

$$L_{13} = L_{31} = \frac{1}{4}\gamma\left(2 + \cos^2 \alpha\right) + \frac{3}{4}\gamma' \sin^2 \alpha \tag{12}$$

and

$$L_{12} = L_{21} = L_{23} = L_{32} = \frac{1}{4}\gamma + \frac{1}{4}\gamma'\left(1 + \cos^2 \alpha\right) \tag{13}$$

Similarly, the two central components at ω_o and ω_o' have the same width L_c equal to:

$$L_c = \frac{1}{2}\gamma + \frac{1}{2}\gamma' \sin^2 \alpha. \tag{14}$$

In C-T&R, the exact reasons why the width of *each* dressed-atom fluorescent transition depends upon the widths of *both* bare-atom fluorescent transitions are carefully explained.

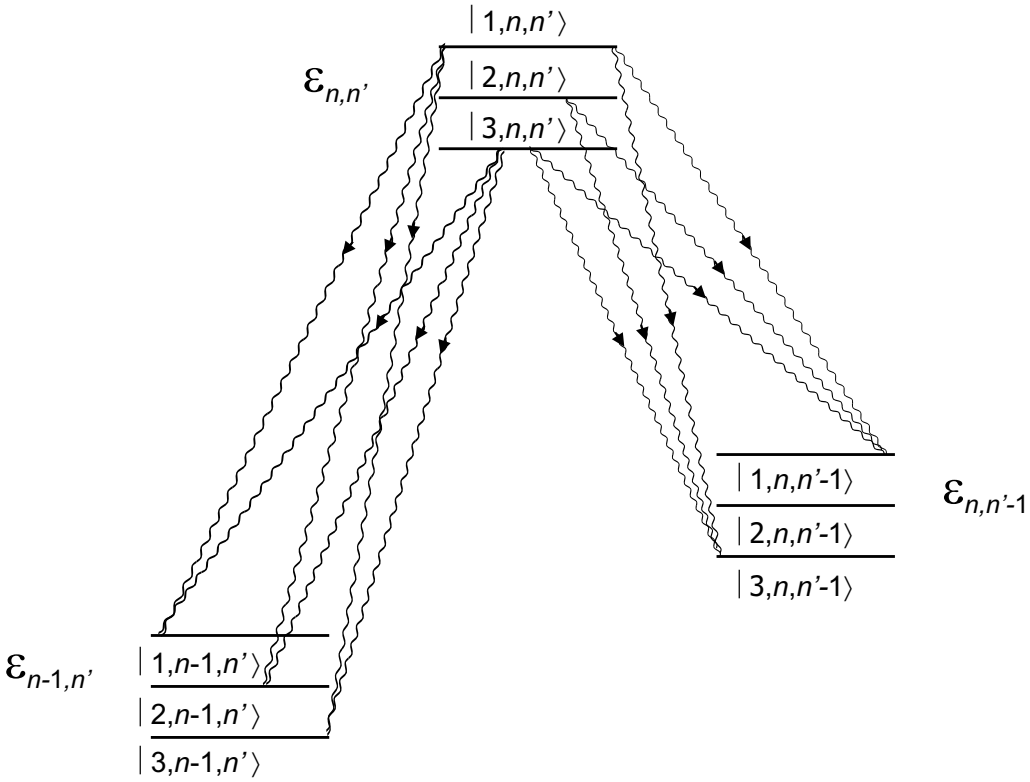

Fig. 16. Diagram showing all spontaneous emission decays (wavy arrows) which are allowed from the three perturbed states of $\varepsilon_{n,n'}$ to lower multiplicities in cascade-type dressed atoms. After Fig. 6 of Cohen-Tannoudji & Reynaud (1977).

To obtain the strengths of either the dressed-atom fluorescence or the dressed-atom absorption components, one needs to know the equilibrium populations π_i of the dressed-atom states (see Eq. (2)). Under the so-called “secular approximation” ($\Omega_1 \gg \gamma, \gamma'$), C-T&R show that the π_i can be obtained from simple rate equation considerations. The steady-state solution to these equations is found to be

$$\pi_1 = \pi_3 = \frac{\gamma' \cos^2 \alpha}{\gamma \sin^2 \alpha + 2\gamma' \cos^2 \alpha} \tag{15}$$

$$\pi_2 = \frac{\gamma \sin^2 \alpha}{\gamma \sin^2 \alpha + 2\gamma' \cos^2 \alpha} \tag{16}$$

With use of both Fig. 16 and Eqs. (15, 16), it is straightforward to predict the general appearance of absorption spectra of dressed cascade-type atoms.

For definiteness, let it be assumed that the ratio of the Rabi frequencies of the resonant laser beams applied to the three-level atomic gas is such that $\pi_2 > \pi_1 = \pi_3$. Then the only absorption present about the *ab* transition occurs in two bands at $\omega_o \pm (1/2)\Omega_1$. No absorption occurs at ω_o because of the essential equality of the populations in, for example, the states $|\, 3, n-1, n'\rangle$ and $|\, 3, n, n'\rangle$. This of course simply reflects the fact that a condition of EIT automatically results from the presence of both applied resonant laser beams. From Fig. 16, it is apparent that EIT is equivalent to “saturation“ occurring on transitions between dressed-atom states. For similar reasons, there is no absorption at $\omega_o \pm \Omega_1$. If the power in the two resonant laser beams is

increased in such a manner that the angle α remains constant, the strengths of the two absorption bands will remain the same, but the frequencies of the peaks will shift further away from ω_o. *It is therefore clear that the dressed-atom linear absorption spectrum near ω_o does not saturate as the power in the two resonant laser beams becomes very high.*

Consider next what happens in Fig. 16 on transitions close to ω_o', still under the assumed condition $\pi_2 > \pi_1 = \pi_3$. Here it is apparent that there is only gain - no absorption - in the only nonsaturated bands present, the ones at $\omega_o' \pm (1/2)\Omega_1$. Any blackbody continuum flux that is resonant with these transitions can only drive stimulated emission processes that add photons to the continuum, but *remove* them from the coherent laser beam at ω_o'. One therefore concludes that, with a cascade-type dressed-atom gas, continuum light can be absorbed about only one of the two bare-atom transitions, while near the other it can only be amplified. Assuming $\pi_2 < \pi_1 = \pi_3$ doesn’t change this conclusion, as can be seen from Fig. 16. In Sect. 4, it will be seen that for Λ-type and V-type dressed-atom gases, only absorption occurs in the vicinities of both bare-atom transitions.

4. Spectral properties of Λ-type and V-type dressed-atom gases

In Narducci et al. (1990) the spontaneous emission and absorption properties of driven V-type three-level systems are calculated in considerable detail. General case formulas are derived that apply when the secular approximation ($\Omega_1 >> \gamma, \gamma'$) is not valid, but a dressed-state description closely following the approach of C-T&R for the high-intensity limit is also included. In a subsequent paper (Manka et al. 1977), several of whose authors also contributed to Narducci et al. (1990), corresponding spectral properties of the Λ and cascade models were investigated. The formulas for emission and absorption in the high-intensity limit contained in both of these papers generally agree with what can be discerned about driven three-level systems via inspection of dressed-atom energy level diagrams such as the one shown in Fig. 16. For example, formulas given in Manka et al. (1977) for the absorption spectra of the cascade model in the high intensity limit verify the conclusion drawn in Sect. 3 that absorption can be obtained in the vicinity of one transition, but not both.

For the Λ system (Fig. 1c), we are here again interested in the high-intensity limit. Application of the two resonant laser fields again lifts the degeneracies of the multiplicities $\varepsilon_{n,n'}$, splitting them in exactly the same manner as shown in Fig. 15. Analagous to Eqs. (11) are equations expressing the dressed-atom wavefunctions as linear combinations of the bare-atom wavefunctions for the Λ system:

$$
\begin{aligned}
|\,1,n,n'\rangle &= \frac{1}{\sqrt{2}}\left(\cos\alpha\,|\,a,n+1,n'\rangle + |\,b,n,n'\rangle\right) \\
&\qquad + \frac{1}{\sqrt{2}}\left(\sin\alpha\,|\,c,n,n'+1\rangle\right) \\
|\,2,n,n'\rangle &= -\sin\alpha\,|\,a,n+1,n'\rangle + \cos\alpha\,|\,c,n,n'+1\rangle \qquad (17) \\
|\,3,n,n'\rangle &= \frac{1}{\sqrt{2}}\left(\cos\alpha\,|\,a,n+1,n'\rangle - |\,b,n,n'\rangle\right)
\end{aligned}
$$

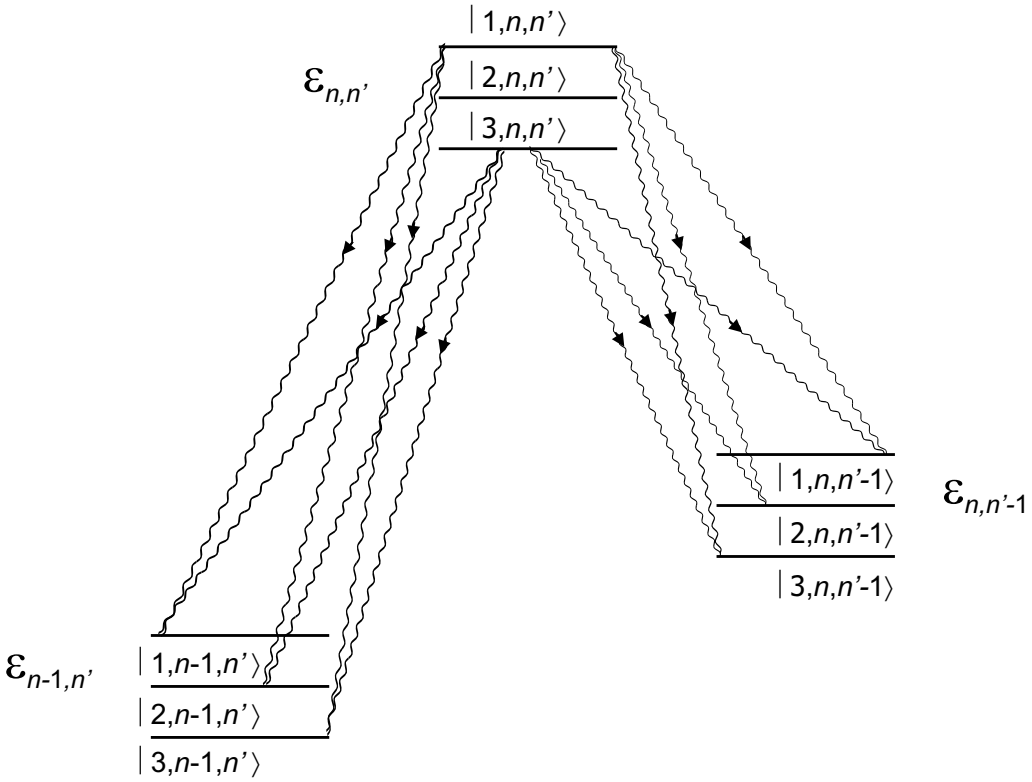

Fig. 17. Diagram showing all spontaneous emission decays which are allowed from the three perturbed states of $\varepsilon_{n,n'}$ to lower multiplicities in Λ-type dressed atoms.

$$+\frac{1}{\sqrt{2}}\left(\sin\alpha \mid c, n, n'+1\right\rangle)$$

Following the same procedure which led to the construction of Fig. 16, one can prepare an analagous diagram for the Λ system showing all the allowed spontaneous emission transitions that can occur from a given multiplicity $\varepsilon_{n,n'}$ (Fig. 17). It is apparent from Fig. 17 that, for the Λ system, the pattern of allowed spontaneous emissions around both bare-atom frequencies is the same as that around the *ab* transition for cascade-type dressed atoms. However, the equations for the Λ system that are analagous to Eqs. (15, 16) for the cascade system are very much simpler. Simply by inspecting Fig. 17 one can see at once that, under the secular approximation, the following must hold: $\pi_1 = \pi_3 = 0$; $\pi_2 = 1$. The presence of applied laser beams at both ω_o and ω_o' has thus resulted in all the atoms in the gas becoming “coherently trapped” in the $\mid 2, n, n'\rangle$ dressed-state levels. Moreover, this occurs for all values of tan α, the ratio of the individual laser Rabi frequencies (Eq. 6).

From inspection of Fig. 17, one can also instantly see why no fluorescence is emitted from a Λ-type dressed-atom gas. As is by now well known to scientists in the quantum electronics field, coherent trapping of Λ-type systems can be vividly demonstrated in the laboratory as a complete quenching of fluorescent emission from (bare-atom) level *b* when both laser beams are applied to a vapor cell, whereas when only one or the other of the beams is applied, bright fluorescence is seen. Among the earliest papers to discuss coherent trapping of Λ-type dressed atoms and to

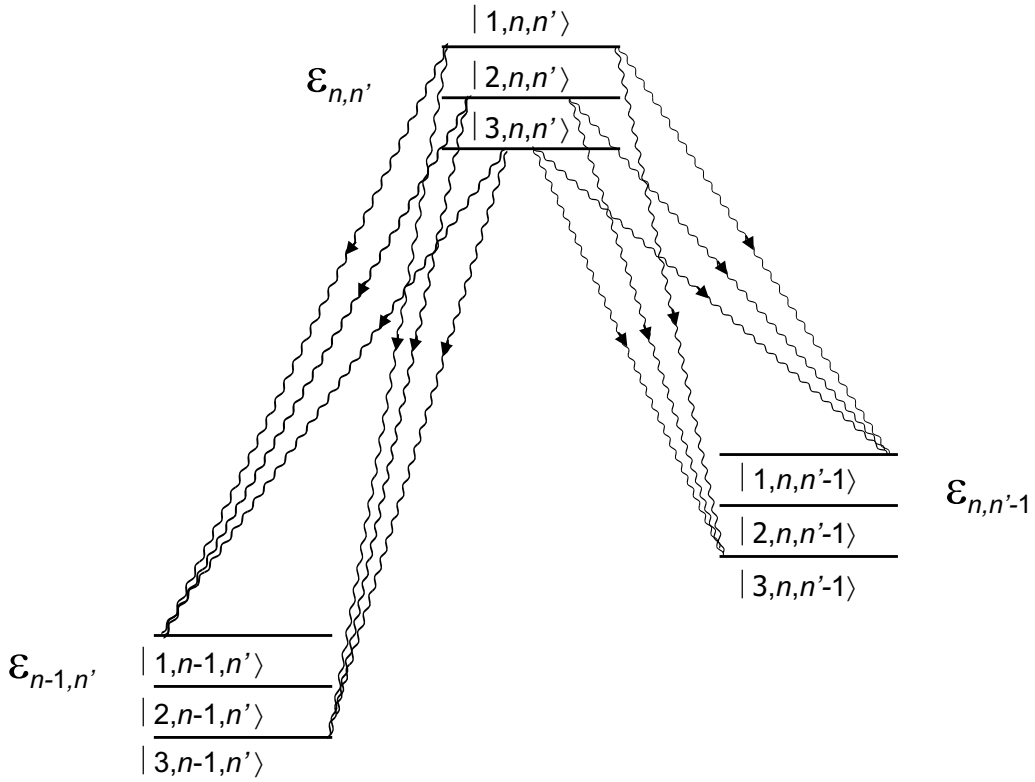

Fig. 18. Diagram showing all spontaneous emission decays which are allowed from the three perturbed states of $\varepsilon_{n,n'}$ to lower multiplicities in V-type dressed atoms.

report laboratory demonstrations of this effect were Alzetta et al. (1976), Arimondo and Orriols (1976), and Gray et al. (1978).

Again, from mere inspection of Fig. 17, one can see that the linear spectrum of Λ-type dressed atoms consists only of absorption bands at $\omega_o \pm (1/2)\Omega_1$ and $\omega_o' \pm (1/2)\Omega_1$. No linear gain is present around either of the bare-atom frequencies.

Figure 18 shows the analagous spontaneous emission diagram for V-type dressed atoms. Here the pattern of allowed spontaneous emission transitions about each bare atom frequency is seen to be the same as that about the *bc* transition in cascade atoms. The steady state solution for the dressed-atom level populations can be deduced from inspection of this figure to be $\pi_1 = \pi_3 = 1/2$, $\pi_2 = 0$, and this again holds for all intensity ratios of the two applied laser beams. The term “coherently trapped atoms” is therefore also a fitting description for V-type dressed atoms. The fluorescence spectrum in this case consists of a triplet around each of the bare-atom frequencies, with components at ω_o, $\omega_o \pm \Omega_1$, ω_o', and $\omega_o' \pm \Omega_1$. The linear spectrum of the dressed atoms here again contains only absorption bands occurring at $\omega_o \pm (1/2)\Omega_1$ and $\omega_o' \pm (1/2)\Omega_1$.

5. Stimulated hyper-Raman scattering (SHRS): a realistic nonlinear mechanism for continuum pumping of dressed-atom space lasers

One can utilize either Fig. 17 or Fig. 18 to evaluate possible pumping mechanisms for Λ- or V-type dressed-atom space lasers, respectively. For the sake of definiteness, we here consider how

amplification can be achieved in a gas of V-type dressed atoms irradiated by a continuum flux comparable to that emitted at the surface of the hot white dwarf in a symbiotic star.

In the absence of a very high electron density n_e (*vide infra*), there are only three optical pumping mechanisms which potentially could provide amplification for both applied laser beams in a dressed-atom space laser: linear pumping by the continuum light, stimulated broadband Raman scattering (SRS), and stimulated hyper-Raman scattering (SHRS). Consider first the effect of linear pumping via absorption of continuum light in the dressed-atom bands at $\omega_o \pm (1/2)\Omega_1$. An individual photonic event that occurs in this type of process might be, for example, absorption of a continuum photon at $\omega_o - (1/2)\Omega_1$ accompanied by excitation of a dressed atom from state $|\, 1, n-1, n'\rangle$ to state $|\, 2, n, n'\rangle$. While through this event the photon number in the laser mode at ω_o is temporarily increased by 1, the energy thus gained by the dressed-atom system soon becomes irretrievably lost via the four fluorescent transitions indicated in Fig. 18. The rate at which dressed atoms are excited from $|\, 1, n-1, n'\rangle$ to $|\, 2, n, n'\rangle$ via linear absorption is given by the continuum flux within the dressed-atom absorption bandwidth times the maximum absorption cross-section. In Sect. 2, it was estimated that at 1000 Å the continuum intensity at the surface of the hot white dwarf in a symbiotic star was ~16.4 W/cm^2 in a 160 MHz (0.005 cm^{-1}) bandwidth. Since 160 MHz is the natural linewidth of an allowed transition that radiatively decays in 1 ns, an upper limit to the continuum flux within the dressed-atom absorption bandwidth would thus be ~8 x 10^{18} photons/cm^2 sec. Taking the maximum cross-section of the dressed-atom absorption band to be $\lambda^2/2\pi = 1.6 \times 10^{-11}$ cm^2, the rate of continuum-driven linear excitation from $|\, 1, n-1, n'\rangle$ to $|\, 2, n, n'\rangle$ would be no greater than ~1.3 x 10^7 sec^{-1}, which is significantly less than the net rate of fluorescent decay from $|\, 2, n, n'\rangle$. Thus, one must look beyond linear absorption to find an effective dressed-atom space laser pumping mechanism.

Consider next stimulated Raman scattering (SRS) as a possible pumping mechanism for dressed-atom space lasers. SRS is a stimulated two-photon process that efficiently converts pump light into coherent light called the Stokes wave. It works equally well whether or not the pump light is coherent (*vide infra*). In SRS, the unit step involves simultaneous absorption of a pump photon and creation of a Stokes-wave photon, with an atom moving from a populated initial level to an unpopulated terminal level, and with total energy being exactly conserved in the step. From the V-type dressed-atom energy diagram (Fig. 18), one sees that four separate SRS photonic processes which generate Stokes waves at the bare-atom frequencies are theoretically possible. One such process would involve the simultaneous absorption of a continuum photon at $\omega_o - (1/2)\Omega_1$ accompanied by the emission of a photon at ω_o. From Fig. 18, one sees that such SRS events would originate from populated dressed-atom $|\, 1, n, n'\rangle$ levels and terminate on unpopulated dressed-atom $|\, 2, n, n'\rangle$ levels. Light at ω_o would also be generated via the SRS process in which continuum light at $\omega_o + (1/2)\Omega_1$ is absorbed. Here the events would originate from populated $|\, 3, n, n'\rangle$ levels and terminate again on unpopulated $|\, 2, n, n'\rangle$ levels. Two similar SRS transitions occurring about ω_o' could, in principle, provide amplification at that frequency. All four SRS processes must originate from the upper levels shown in Fig. 18 in order to terminate

on unpopulated levels. There are also four potential SRS processes starting from the upper levels that terminate on unpopulated levels but have Stokes-wave frequencies different from the bare-atom frequencies. These would, however, be discriminated against, because the SRS transition probability is proportional to the instantaneous power in the Stokes wave, and the latter can only build up if the Stokes-wave frequency stays constant.

In the above discussion, the effective SRS pump radiation and the Stokes-wave emission were considered to be exactly centered on resonances. However, SRS pumping in a space laser would most likely occur as *broadband* SRS, an effect known in the quantum electronics field for more than thirty years. The first experimental broadband SRS study reported appears to have been that of Bocharov et al. (1969). The first theoretical discussions of this effect appeared in D’yakov (1970) and in Carman et al. (1970). Other early broadband SRS studies are referenced in Bethune et al. (1979). Generally, in the nineteen seventies, scientists began to observe in various experiments that there was a large forward-backward asymmetry of the Raman gain when broadband pump lasers were used. As noted in Raymer et al. (1979), “These asymmetries are consistent with several predictions (Carman et al. 1970, Akhmanov et al. 1974) that in the backward direction (counterpropagating pump and Stokes waves) the gain coefficient is proportional to $(\Gamma + \Gamma_L)^{-1}$, where Γ and Γ_L are the spectral widths of the Raman medium and the pump laser, respectively; while, in the forward direction, in the absence of dispersion of the Stokes wave relative to the pump wave, the gain is proportional to Γ^{-1} alone.” Raymer et al. (1979) then note that Carman et al. (1970) refer to this as “the rather startling conclusion... that the Stokes gain is independent of the frequency spectrum of the (pump) laser... even if this spectrum is much broader than Γ.” Raymer et al. (1979) then continue: “Thus when Γ_L is much larger than Γ, the forward gain is much larger than the backward gain. These results go against intuition based on the idea that gain should depend on the number of photons per unit frequency in the pump beam. Apparently, the concept of photons as independent incoherent bundles is inadequate to describe the subtleties in the SRS problem.”

In the case of the symbiotic star space laser model that was proposed in Sect. 2, the pump and dressed-atom-laser radiation were assumed to be copropagating, so that the pump-laser beam geometry is indeed an optimum one for broadband SRS to occur. One important thing to keep in mind about broadband SRS is that the bandwidth of the Stokes light generated will usually equal that of the pump light absorbed. Another important point regarding this nonlinear photonic process, one that was already highlighted in the previous paragraph, is that if, as shown in Fig. 19, the pump spectrum doesn’t actually overlap the transition from the initial state (1) to the intermediate state (2), then the threshold for SRS is completely independent of the pump bandwidth, and just depends upon the total pump power. Scientists in the quantum electronics field frequently explain such bandwidth-independent SRS threshold behavior, and also the fact that SRS can evidently be excited just as easily by incoherent light as by coherent light, by postulating that, whenever SRS does occur, the Stokes-wave radiation is generated with a time-varying phase that exactly equals the time-varying phase of the pump radiation, no matter how randomly-varying

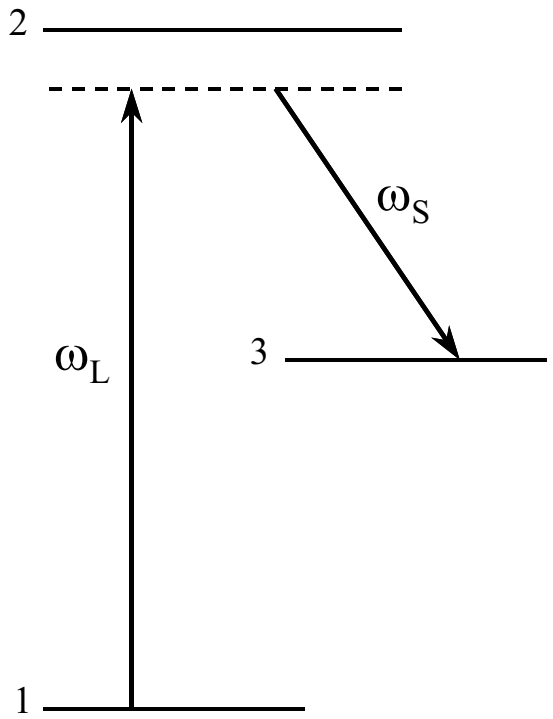

$$E_L = \varepsilon_L \cos\left(\omega_L t - k_L z + \varphi_L\right)$$
$$E_S = \varepsilon_S \cos\left(\omega_S t - k_S z + \varphi_S\right)$$
Phase locking occurs when $\varphi_S\left(z,t\right) = \varphi_L\left(z,t\right)$.

Fig. 19. Diagram of a broadband SRS process in which the pump beam spectrum is offset from the intermediate state resonance. The phase $\phi_L(z,t)$ of the pump beam electric field is here assumed to be stochastically varying.

the latter may be (c.f. the equations shown in Fig. 19). This is the so-called “phase locking” postulate. However, according to Raymer et al. 1979, its theoretical basis is not particularly well understood. When the equations in Fig. 19 are substituted into the nonlinear equations describing the growth of the Stokes wave in SRS, the phases of the pump and Stokes-wave fields exactly cancel, and do not therefore enter at all into the determination of the SRS Stokes-wave gain, and hence threshold value. However, a pump field E_L in Fig. 19 having a constant amplitude ε_L but a stochastically-varying phase ϕ_L which abruptly changes at a rate $\dot{\phi}_L = 2\Gamma_L$ would have a spectral bandwidth of Γ_L, and could therefore potentially possess a very “broadband” spectrum. This is the so-called “phase diffusion” model of stochastic light. It is frequently employed in nonlinear optics calculations (e.g. in Raymer et al. 1979 and in references cited in that work), because the mathematics involved is relatively tractable. We note in passing that, at first glance, this model would also seem to be a reasonable one with which to represent the thermal continuum light emitted by a hot star.

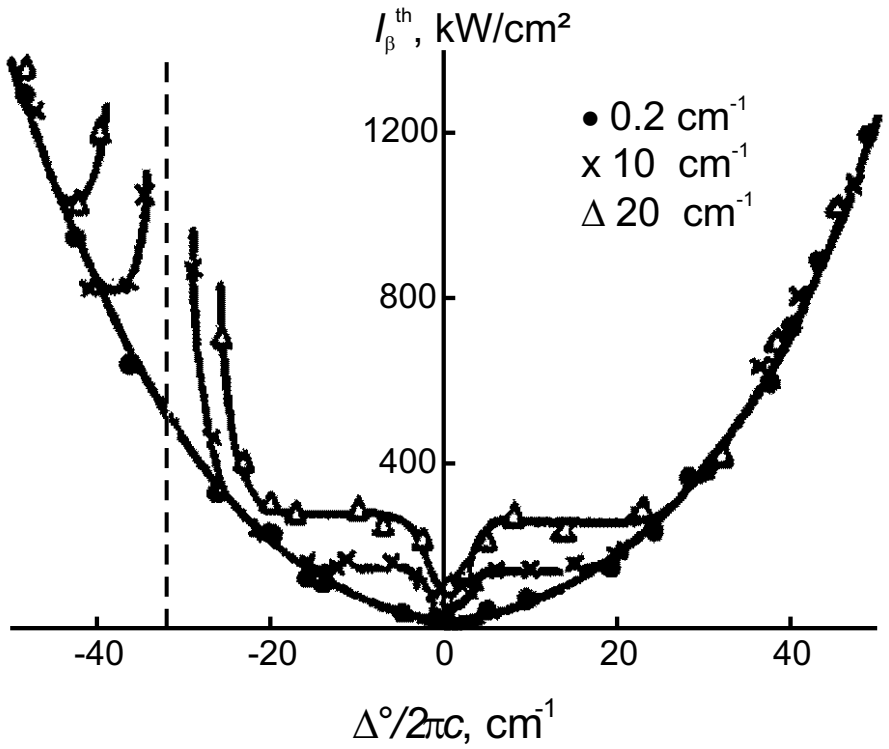

Fig. 20. Experimental measurements by Korolev et al. (1978) showing the dependency of SRS threshold on both the center frequency and bandwidth of the pump beam spectrum, when the latter overlaps the intermediate state resonance. The pump beam bandwidths utilized are indicated. After Fig. 2 of Korolev et al. (1978).

For a pump spectrum that doesn’t overlap the intermediate state resonance (Fig. 19), the SRS threshold varies as the square of the frequency offset. When the pump spectrum overlaps the intermediate state resonance, the SRS threshold depends upon the *spectral density* of the pump, and one sees a threshold dependence as shown in Fig. 20.

Basically, all the above facts about broadband SRS are consistent with it occurring in a gas of V-type dressed atoms irradiated by a strong continuum. For example, under the assumption that phase locking occurs in SRS, it can easily be shown that a certain nonlinear photonic loss process - one that *a priori* would seem to have the potential to cancel entirely the laser gain produced by SRS - can actually be neglected. This is *two-photon absorption* (TPA). In the V-type dressed-atom diagram (Fig. 18), the TPA process could be represented, for example, by a simultaneous two-photon absorption step originating from $|\,3, n-1, n'\rangle$, proceeding upwards via $|\,3, n, n'\rangle$, and terminating on $|\,2, n+1, n'\rangle$. However, whereas the randomly-varying pump and Stokes-wave phase shifts cancel in SRS, they add in TPA. This continually keeps the sum of the pump and Stokes-wave photon energies detuned from the two-photon resonance, thus lowering the TPA transition probability.

However, as stated earlier, there are completely obvious reasons why broadband SRS simply cannot be the photonic pump mechanism responsible for the superintense O VI FUV emission observed in symbiotic stars. In broadband SRS, the spectral width of the continuum radiation

absorbed would necessarily have to equal exactly the spectral width of the Stokes-wave radiation that is generated. Since the number of Stokes-wave photons generated per unit time would also have to equal exactly the number of continuum photons absorbed per unit time, and since both absorption and emission would here occur over roughly the same spectral region, it is apparent that one should actually never be able to detect the presence of broadband SRS in a space object, even if it were occurring. This therefore would appear to leave only stimulated hyper-Raman scattering (SHRS) to be considered as a possible pumping mechanism for a dressed-atom laser in a space object such as RR Tel, where the narrow-band emission intensity as seen from Earth is some 600 times more intense than the continuum level. We now explore this idea in some detail.

Figure 21 is a schematic diagram showing the basic SHRS processes which are assumed to occur around *both* bare-atom frequencies ω_o and ω_o' in a dressed-atom space laser, although only processes around the former frequency are shown. The two photonic processes shown at the left would generate photons at ω_o. The two processes shown at the right are competing ones, which would act to remove photons at ω_o from the generated Stokes wave. As stated above, and as can be seen from Fig. 18, there are equivalent processes that occur around ω_o'. As can also be seen from Fig. 18, there are various “cross processes” that can occur. An example of the latter would be the following: Starting with an atom in $|\,3, n-1, n'\rangle$, a continuum photon at $\omega_o + \Omega_1 + \Delta$ is absorbed, a photon at ω_o' is emitted, and a continuum photon at $\omega_o' - \Omega_1/2 - \Delta$ is absorbed, with all events occurring simultaneously and with the atom ending up in the unpopulated level $|\,2, n, n'\rangle$. In Fig. 21, the value of Δ is arbitrary, and in principle could extend out to values $\sim \omega_o/2$, or more. However, the cross-section σ_{SHRS} for the hyper-Raman scattering process varies as $1/\Delta^4$ (Hanna et al. 1976). Such a steep fall-off of σ_{SHRS} with Δ at once implies that the SHRS mechanism would be incapable of harvesting continuum light at frequencies greatly offset from ω_o and ω_o', and converting it into narrow-band light at the latter frequencies. It was shown in Sect. 2 that in symbiotic stars, at least, any viable dressed-atom laser pumping mechanism must nonetheless possess this capability. Later on in this section, a solution to this seemingly insurmountable conceptual difficulty will be proposed. It is first, however, necessary to indicate why the SHRS gain processes shown at the left in Fig. 21 might be more important than the loss processes shown at the right.

The following argument is based upon the assumption that, when a stimulated hyper-Raman scattering process occurs, the phases of the three participating waves are related in a manner analagous to the condition $\phi_L(z,t) - \phi_S(z,t) = 0$ linking the phases of the pump and the generated Stokes-wave light in broadband SRS (Fig. 19). Considering the waves participating in the SHRS processes shown in Fig. 21, and also those (not shown in Fig. 21) which involve frequencies around ω_o', one would write:

$$\phi_c\,(\omega_o + \Omega_1 + \Delta) - \phi(\omega_o) + \phi_c(\omega_o - \Omega_1/2 - \Delta) = 0, \tag{18a}$$

$$\phi_c\,(\omega_o - \Omega_1 - \Delta) - \phi(\omega_o) + \phi_c(\omega_o + \Omega_1/2 + \Delta) = 0, \tag{18b}$$

$$\phi_c\,(\omega_o + \Omega_1 + \Delta) - \phi(\omega_o') + \phi_c(\omega_o' - \Omega_1/2 - \Delta) = 0, \tag{18c}$$

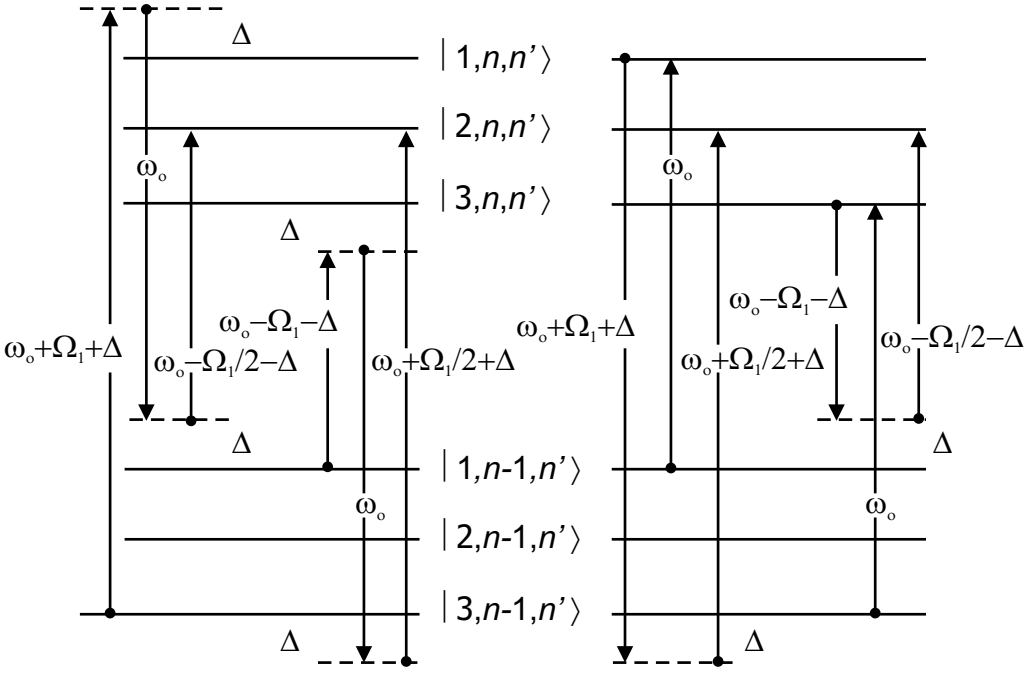

Fig. 21. Schematic diagram showing the basic SHRS processes which are assumed to occur around both bare-atom frequencies ω_o and ω_o' in a dressed-atom space laser. (Only processes around the former frequency are shown.) The two processes shown at the right are competing ones (see text).

$$\phi_c\,(\omega_o - \Omega_1 - \Delta) - \phi(\omega_o') + \phi_c(\omega_o' + \Omega_1/2 + \Delta) = 0, \tag{18d}$$

$$\phi_c\,(\omega_o' + \Omega_1 + \Delta) - \phi(\omega_o') + \phi_c(\omega_o' - \Omega_1/2 - \Delta) = 0, \tag{18e}$$

$$\phi_c\,(\omega_o' - \Omega_1 - \Delta) - \phi(\omega_o') + \phi_c(\omega_o' + \Omega_1/2 + \Delta) = 0, \tag{18f}$$

$$\phi_c\,(\omega_o' + \Omega_1 + \Delta) - \phi(\omega_o) + \phi_c(\omega_o - \Omega_1/2 - \Delta) = 0, \tag{18g}$$

$$\phi_c\,(\omega_o' - \Omega_1 - \Delta) - \phi(\omega_o) + \phi_c(\omega_o + \Omega_1/2 + \Delta) = 0, \tag{18h}$$

with $\phi_c(\omega)$ being the phase of a small bandwidth of continuum light at ω used in pumping the various SHRS processes.

From Eqs. (18c) and (18e), it follows that $\phi_c\,(\omega_o + \Omega_1 + \Delta) = \phi_c\,(\omega_o' + \Omega_1 + \Delta)$. From Eqs. (18d) and (18f), it likewise follows that $\phi_c\,(\omega_o - \Omega_1 - \Delta) = \phi_c\,(\omega_o' - \Omega_1 - \Delta)$. Since Δ is of arbitrary value, it then follows from (for example) Eqs. (18a) and (18b) that $\phi(\omega_o) = \phi(\omega_o')$. *This last equation represents a necessary and sufficient condition for the atoms to remain “dressed” as the light intensity at both narrow band frequencies ω_o and ω_o' continues to increase due to SHRS.*

By contrast, for the first of the two competing processes shown at the right in Fig. 21 to be correctly phased for optimum transition probability, one would require $\phi(\omega_o) - \phi_c\,(\omega_o + \Omega_1 + \Delta) + \phi_c(\omega_o + \Omega_1/2 + \Delta) = 0$. From Eq. (18a), this would then require that $\phi_c(\omega_o - \Omega_1/2 - \Delta) = -\phi_c(\omega_o + \Omega_1/2 + \Delta)$. Since this last equation does not follow from Eqs. (18a - 18h), one is able to conclude that rapid phase fluctuations of the waves involved in the competing process keep

it continually detuned from exact three-photon resonance, thus greatly decreasing its transition probability. The reader will recognize that this argument is essentially the same as the one used earlier to show that TPA could be neglected in the case of broadband SRS.

The seriousness of the rapid fall-off of SHRS transition probability with Δ must now be addressed. On the basis of the SHRS photonic mechanism acting *alone*, there is *a priori* no possibility for continuum light photons at frequencies which are thousands of wavenumbers offset from ω_o and ω_o' to be harvested and converted into narrow-band light at these same two frequencies. Yet in Sect. 2, evidence was presented to show that, at least in symbiotic star systems, exactly this process must occur. The authors are currently able to propose one mechanism that potentially could aid in enabling efficient transfer of continuum photon energy over such large spectral intervals in symbiotic stars to be achieved. That mechanism, if it is a truly realizable one, would probably best be termed *stimulated (or induced) hyper-Compton scattering (SHCS)* and will now be briefly discussed.

Spontaneous Compton scattering (also known as Thomson scattering) involves single photon scattering by electrons. As shown in physics textbooks, in order for both energy and momentum to be conserved in each scattering event, the wavelength of the outgoing photon can differ only slightly from that of the incident photon. At 1000 Å, the maximum shift would be only $\simeq 2.5$ cm^{-1}, so that transfer of continuum photon energy over large spectral intervals is unlikely via this mechanism. The cross-section for Thomson scattering is also fairly small: $\sigma_T = 6.6 \text{ x } 10^{-25}$ cm^2. The net rate of Thomson scattering is proportional to the electron density n_e. In the O VI regions of symbiotic stars, n_e can be of the order of 10^{10} cm^{-3}, this value approximately representing the density of H atoms in the spherically symmetric solar wind emanating from the red giant.

An increase in the Compton scattering rate can occur as a result of *stimulated* (or *induced*) Compton scattering (see, for example, Wilson 1982). Here the rate is proportional both to n, the photon occupation number of the initial state, and to $(1 + n_1)$, where n_1 is the (initial) photon occupation number in the new state. In stimulated Compton scattering, the basic spontaneous Compton scattering rate is therefore enhanced by orders of magnitude by the product nn_1. However, in each event only a very small amount of photon energy is still exchanged. Stimulated Compton scattering was invoked in Montes 1977 to explain the presence of intensity “relaxation oscillations” observed in some OH and H_2O interstellar maser lines.

We here propose that a multi-photon version of stimulated Compton scattering can occur in the O VI regions of symbiotic stars. In the unit step of the envisioned process, two continuum photons, offset equally to low and high frequencies from the O VI doublet (here represented, for simplicity, by a single line at ω_o), impinge upon a single electron and are simultaneously scattered. Two new photons at ω_o are simultaneously produced. Both energy and momentum are conserved in this photonic exchange, and the energy and momentum of the electron therefore remains about the same. Consequently, the cross-section of this process should roughly be independent of Δ, the absolute value of the frequency offset from ω_o of the two continuum photons being scattered. The total rate of such events occurring in a symbiotic star O VI region will

be proportional to the product of n_e, $I(\omega_o)$, and I_c^2, where I_c is the continuum photon intensity. By analogy with SHRS, such a process could logically be termed stimulated hyper-Compton scattering (SHCS).

If it existed, SHCS would have the desired effect of efficiently shifting continuum photons that are spectrally very remote from ω_o into the immediate spectral vicinity of the latter, from where they could be absorbed with high probability by SHRS and converted into properly phased coherent radiation at the O VI doublet frequencies. One is compelled to postulate that SHCS occurs in symbiotic star dressed-atom lasers because of the large value (~600) of the O VI doublet-to-continuum intensity ratio observed in these systems.

It was noted in S&G I that the presence of Doppler broadening is known to increase generally the difficulty of maintaining a condition of EIT in a spectral region spanning one of the bare-atom transitions (the “probe beam” transition) in a three-level gas, when an intense monochromatic laser beam is applied to the other bare-atom transition (the “coupling beam” transition). This is illustrated by the calculations shown in Fig. 22. Consider the transparency curves which are plotted in this figure for V-type systems (Fig. 22c). When the probe frequency is greater than the pump frequency ($\lambda_c > \lambda_p$), incomplete transparency is seen to be produced about the former transition. The transparency induced when $\lambda_c > \lambda_p$ is even much less in the cases of cascade- and Λ-type systems (Figs. 22a and 22b). Since, in any three-level dressed-atom laser, a condition of high transparency must exist about *both* bare-atom transition frequencies in order that there be net gain present at both frequencies, it is at once apparent from this figure that *the lowest thresholds for dressed-atom space lasers should exist in V-type systems having approximately equal bare-atom frequencies.* The O VI bare-atom frequencies are very close together, and this may therefore be a contributing reason why emission from this system is observed to be so dominant in symbiotic stars.

6. Summary: main features of the symbiotic star dressed-atom laser model

A model is proposed for a type of space laser which potentially can account for superintense narrow-band visible/UV/FUV radiation emitted from certain objects in Space. The model comprises a rarifed, three-level, dressed-atom gas situated near an extremely hot illuminating source. In the present paper attention is specifically focussed on using this model to explain the origin of the superintense (1032 Å, 1038 Å) emission doublet that dominates the FUV spectra of symbiotic stars such as RR Tel.

In the symbiotic star laser model, the amplifying medium is a gas of O VI ions located in a spherical region (radius l) centered on the hot (T ~ 180000°K), relatively tiny ($R_h \sim 0.04 R_\odot$), white dwarf member of a symbiotic pair. The O VI ions are produced through photoionization of O atoms contained in a constant velocity, spherically symmetrical, wind (H-atom density ~ 10^{10} cm^{-3}) that emanates from the red giant photosphere, with the ionizing source being the hot white dwarf thermal continuum. Within the radius l, the O VI ion density would therefore be ~10^4-10^5

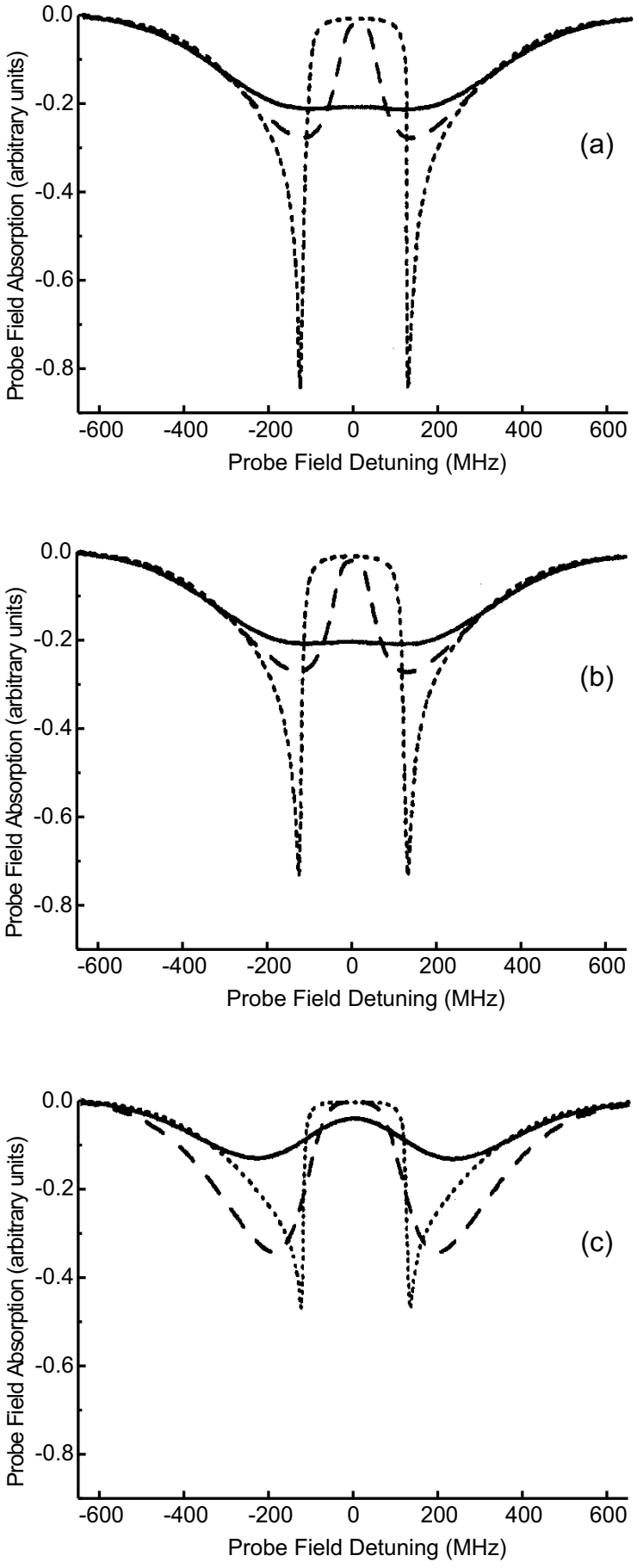

Fig. 22. Absorption of a weak probe field as a function of detuning for (a) the cascade, (b) the Λ, and (c) the V-type schemes. A resonant coupling field with Rabi frequency (= 250 MHz) equal to half the Doppler width (= 500 MHz) is assumed present. In each case, three wavelength regimes are considered: $\lambda_c<\lambda_p$ (dotted line), $\lambda_c = \lambda_c$ (dashed line), and $\lambda_c>\lambda_p$ (solid line). Reproduced from Fig. 2 of Boon et al. (1999).

cm^{-3}, and the electron density n_e would be $\sim 10^{10}$ cm^{-3}. The radius l would be on the order of several times R_h.

In the model, a dressed-atom laser beam, comprising narrow-band radiation centered at both 1032 Å and 1038 Å, originates near the white dwarf surface and propagates towards the red giant, becoming greatly amplified as it does so. The laser field would have cylindrical symmetry about the line that joins the two stars, and be largely confined within some angle θ about this line. All the dressed-atom laser beam amplification would occur within a radius l of the white dwarf.

Energy to pump the dressed-atom laser is provided by the white dwarf thermal continuum radiation emitted in the direction of the red giant. During the early stages of laser beam amplification, the photonic mechanism through which incoherent thermal continuum light is converted into coherent light at both O VI bare-atom frequencies is stimulated hyper-Raman scattering (SHRS). As the intensity of the laser light at both frequencies increases, the intrinsic efficiency with which the SHRS pumping process converts continuum light into narrow-band laser light remains constant, i.e. no saturation of the pumping process occurs. This remarkable occurrence results from the combined effect of two separate factors: (1) The integrated linear absorption intensity of a dressed-atom gas remains constant for all power levels of the two monochromatic resonant laser beams that dress the gas. The various dressed-atom absorption bands shift in position, but remain constant in strength. (2) As the SHRS process increases the coherent light intensity at both bare-atom frequencies, it does so in a manner that keeps the atoms “dressed”, by causing the new light that is generated at both frequencies to have the same phase.

Although intrinsic saturation is completely avoided in SHRS pumping of a dressed-atom laser, there is another factor which normally limits the amount of power that can be transferred from the hot star continuum to the dressed-atom laser beam. This stems from the fact that the SHRS cross-section varies as Δ^{-4}, where Δ is the frequency offset from exact resonance of each member of a pair of continuum photons involved in a unit SHRS process (see Fig. 21). This implies that SHRS can only efficiently extract continuum photons having $|\Delta| < \sim 100$ cm^{-1}. When all continuum photons in this range have been depleted via the SHRS pumping process, amplification of the dressed-atom laser beam ceases. To account for the dressed-atom laser beam intensity being several hundred times greater than the background continuum level in a symbiotic star requires conversion of continuum light spanning a very much broader spectral range, e.g. $|\Delta| \sim 20000$ cm^{-1}. It is here postulated that in symbiotic stars this occurs via a specific stimulated multi-photon scattering process in which the scattering particles are electrons, not O VI ions. By analogy with SHRS, this process should be termed stimulated hyper-Compton scattering (SHCS). The transition rate for SHCS would be proportional to the product $n_e \times I(\omega_o) \times I_c^2$, where $I(\omega_o)$ is here the narrow-band dressed-atom laser intensity at either bare-atom resonance frequency, and I_c is the continuum intensity. The probability of SHCS occurring in symbiotic stars would be favored by the large values of n_e which characterize these systems. The SHCS transition rate also depends upon $I(\omega_o)$, and large values of this quantity result from the SHRS-pumped amplification process. We thus speculate that, in a symbiotic star laser, the SHRS process

eventually “triggers” the onset of SHCS, with efficient conversion of continuum photons spanning an enormous spectral range into photons near the bare-atom frequencies then occurring. The photons produced via SHCS could then be efficiently converted to dressed-atom laser photons via SHRS. The advantage of having the latter step occur is that the atoms would remain “dressed” . If such a combined (SHRS, SHCS) process really does occur in symbiotic stars, it would constitute one of the most efficient laser pumping processes known. It was deduced that the maximum intensity of the dressed-atom laser beam in RR Tel must be greater than 100 MW/cm^2.

With an O VI dressed-atom laser beam substituted for the isotropically radiating O VI source assumed in previous models of Raman and Rayleigh scattering in symbiotic stars, one can equally well account for many of the Raman scattering features that are observed. On the basis of such a symbiotic star dressed-atom laser model, the structure observed on the 6825-Å and 7082-Å Raman intensity bands in RR Tel can be easily given an interpretation that is consistent with consensus values of symbiotic star parameters. For example, on the basis of the laser-based model it is deduced that the velocity of the red giant solar wind in this system must be about 38 km s^{-1}, which is in line with values assumed for this parameter in non-laser-based Raman scattering models.

On the basis of Doppler width considerations, it is generally deduced that a dressed-atom laser in Space is far more likely to occur if the bare-atom frequencies of the three-level system are approximately equal. This may partially explain why the O VI FUV doublet emission is so dominant in symbiotic stars.

Acknowledgements. We have benefited from conversations with two colleagues of ours: Drs. R.T. Hodgson and B.E. Elmegreen. We also thank Dr. Elmegreen for kindly allowing us the use of his astronomy journals.

References

Akhmanov, S.A., D’yakov, Yu.E., & Pavlov, L.I. 1974, Sov. Phys. JETP, 39, 249

Alzetta G., Gozzini A., Moi L., et al. 1976,Nuovo Cimento, 36B, 5

Arimondo E., & Orriols G. 1976, Nuovo Cimento Lett., 17, 333

Bethune D.S., Lankard J.R., Loy M.M.T., et al. 1979, IBM J. Res. Develop., 23, 556

Bocharov V.V., Grasyuk A.Z., Zubarev I.G., et al. 1969, Sov. Phys. JETP, 29, 235

Boon J.R., Zekou E., McGloin, D., et al. 1999, Phys. Rev. A, 59, 4675

Carman R.L., Shimuzu F., Wang C.S., et al. 1970, Phys. Rev. A, 2, 60

Cohen-Tannoudji C., & Reynaud, S. 1977, J. Phys. B, 10, 2311

Cohen-Tannoudji C., Dupont-Roc J., & Grynberg, G. 1992, Atom-Photon Interactions (Wiley-Interscience, New York, Chichester, Weinheim, Brisbane, Singapore, and Toronto)

D’yakov Yu. E. 1970, JETP Lett., 11, 243

Espey B.R., Schulte-Ladbeck R.E., Kriss G.A., et al. 1995, ApJ, 454, L61

Ferland G.J. 1993, Univ. Kentucky Phys. Dept. Internal Rep.

Gray H.R., Whitley R.M., & Stroud C.R. 1978, Opt. Lett., 3, 218

Hanna D.C., Yuratich M.A., & Cotter D. 1979, Nonlinear Optics of Free Atoms and Molecules (Springer-Verlag, Berlin, Heidelberg, and New York)

Harries T.J., & Howarth I.D. 1997, A&AS, 121, 15

Jenniskens P., & Désert F.-X. 1994, A&AS, 106, 39

Korolev F.A., Mikhailov V.A., & Odintsov V.I. 1978, Opt. Spectroscopy, 44, 535

Lee K.W., & Lee H.-W. 1997, MNRAS, 292, 573

Manka A.S., Doss H.M., Narducci L.M., et al. 1991, Phys. Rev. A, 43, 3748

Montes C. 1977, ApJ, 216, 329

Moore C.E. 1971, Atomic Energy Levels, Vol. 1, Nat. Stand. Ref. Data Ser., Nat. Bur. Stand. (U.S.), 35

Narducci L.M., Scully M.O., Oppo G.-L., et al. 1990, Phys. Rev. A, 42, 1630

Raymer M.G., Mostowski J., & Carlsten J.L. 1979, Phys. Rev. A, 19, 2304

Sadeghpour H.R., & Dalgarno A. 1992, J. Phys. B, 25, 4801

Schild H., Mürset U., & Schmutz W. 1996, A&A, 306, 477

Schmid H.M. 1989, A&A, 211, L31

Schmid H.M. 1996, MNRAS, 282, 511

Schmid H.M., Krautter J., Appenzellar I., et al. 1999, A&A, 348, 950

Sorokin P.P., & Glownia J.H. 2002, A&A, 384, 350

Webster B.L., & Allen D.A. 1975, MNRAS, 171, 171

Wilson D.B. 1982, MNRAS, 200, 881